PRIAS Personalized Biopsy Schedules

Firstname1 Lastname1

Abstract

Lorem ipsum dolor sit amet, consectetur adipiscing elit. Suspendisse accumsan magna est, quis elementum leo laoreet eu. Donec sollicitudin elit non massa venenatis, in viverra dolor sagittis. Maecenas ac justo pulvinar, consectetur mauris hendrerit, vulputate lacus. Etiam tristique sapien quis sem commodo, et eleifend tortor viverra. In hac habitasse platea dictumst. Phasellus vel tempus risus, sit amet consectetur massa. Duis rutrum lectus eu ligula egestas iaculis. Sed condimentum, ipsum in dignissim condimentum, nisi turpis blandit massa, et aliquam magna ligula eget lacus. Donec ac eleifend nulla, quis cursus nisi. Lorem ipsum dolor sit amet, consectetur adipiscing elit. Suspendisse accumsan magna est, quis elementum leo laoreet eu. Donec sollicitudin elit non massa venenatis, in viverra dolor sagittis. Maecenas ac justo pulvinar, consectetur mauris hendrerit, vulputate lacus. Etiam tristique sapien quis sem commodo, et eleifend tortor viverra. In hac habitasse platea dictumst. Phasellus vel tempus risus, sit amet consectetur massa. Duis rutrum lectus eu ligula egestas iaculis. We demonstrate that personalized schedules are a very promising method to decide biopsy times for prostate cancer patients.

1 Introduction

Prostate cancer is the development of cancer in the prostate gland. With increase in life expectancy and increase in number of screening tests, an increase in diagnosis of low grade prostate cancers has been observed. Majority of these cancers have good long-term survival and in many cases the prostate cancer is (over) diagnosed solely due of screening. i.e. it wouldn't have shown any malignant symptoms for a long time otherwise. To avoid overtreatment, patients diagnosed with prostate cancer are often motivated to join active surveillance (AS) programs instead of taking immediate treatment. The goal of AS programs is to routinely check the progression of prostate cancer and avoid serious treatments such as surgery or chemotherapy as long as they are not needed.

Currently the largest AS program worldwide is PRIAS (www.prias-project.org) (Bokhorst et al., 2015). Patients enrolled in PRIAS are closely monitored using serum prostate-specific antigen (PSA) levels, digital rectal examination (DRE) and repeat prostate biopsies. Biopsies are evaluated using the Gleason grading system. Gleason scores range between 2 and 10, with 10 corresponding to a very serious state of prostate cancer. Patients who join PRIAS have a Gleason score of 6 or less, DRE score of cT2c or less and a PSA of 10 ng/mL or less at the time of induction. Although a PSA doubling time(measured as the inverse of the slope of regression line through the base 2 logarithm of PSA values) of less than 3 years, DRE of cT3 or more, and a Gleason score more than 6 are indicators of prostate cancer progression, only DRE and Gleason scores are considered to be the gold standard in this regard (Bokhorst et al., 2016). If either the DRE or the Gleason score are found to be above the aforementioned threshold, then it is considered that the disease has progressed and the patient is removed from AS for further curative treatment. When the Gleason score becomes greater than 6, it is also known as Gleason reclassification (referred to as GR here onwards).

The reliability of Gleason score comes at a high cost. Biopsies are difficult to obtain, are painful and have serious side effects such as hematuria and sepsis for prostate cancer patients (Loeb et al., 2013). So much so, that PRIAS as well as majority of the AS programs around the world strongly adhere to the rule of not having more than 1 biopsy per year. Performing a biopsy every year has the advantage that it is possible to detect GR within 1 year since its occurrence. The drawbacks of this schedule though, are not only medical but also financial. Keegan et al., 2012 have shown that if a biopsy is performed every year then the costs of AS per head, at 10 years of follow-up

exceed the costs of treatment (brachytherapy or prostatectomy) at 6 and 8 years of follow-up, respectively. They also found that performing biopsy every other year led to 99% increase in savings (AS vs. primary treatment) per head over a period of 10 years compared to the scenario where biopsy is performed every year. Despite this, several AS studies schedule biopsies for every patient annually (Tosoian et al., 2011; Welty et al., 2015). For patients enrolled in PRIAS the schedule is comparatively less rigorous. One biopsy is performed at the time of induction, and the rest are scheduled at 1, 4, 7, 10 years and every 5 years thereafter. For patients who have a PSA doubling time (PSA-DT) less than 10 years, repeat biopsy every year is advised.

The biopsy schedule of PRIAS program is less rigorous than other programs, and yet PRIAS has a high non compliance rate for repeat biopsies. Bokhorst et al., 2015 reported that the percentage of men receiving repeat biopsies decreased from 81% at year 1 to 60% in year 4, 53% in year 7 and 33% in year 10 of follow up. Non compliance of biopsy schedule reduces the effectiveness of AS programs, as progression is detected late. On the other hand even if patients comply with the schedule, be it annually or the schedule of PRIAS, it may not be suitable for them. A patient whose cancer progresses slowly will often end up having biopsies when they are not needed. For a patient who has a faster progressing disease, crude measures such as PSA-DT are employed to decide if frequent biopsies are required. The fact that existing schedules require improvement is also evident in some of the reasons given by patients for non-compliance: 'patient does not want biopsy', 'PSA stable', 'complications on last biopsy'and 'no signs of disease progression on previous biopsy'.

Let us assume that we have a new patient j enrolled in the AS program and let T_j^* denote the actual time of GR for this patient. Let the schedule of biopsies for this patient be given by $\{T_{j0}, T_{j1}, \ldots T_{jN_j^b}\}$, where $T_{jN_j^b}$ is the time at which GR is detected and no further biopsies are conducted. The total number of repeat biopsies conducted till GR is detected is denoted by N_j^b. Because of the periodical nature of biopsy schedules, we only know that $T_j^* \epsilon (T_{jN_j^b-1}, T_{jN_j^b}]$. The most useful biopsy schedule for a patient will be the one with the least number of biopsies N_j^b and the smallest offset $O_j = T_{jN_j^b} - T_j^*$ possible. i.e. the goal is to detect GR as early as possible with minimum possible number of biopsies. The search for the most useful biopsy schedule is the motivation behind this work. To this end, we have proposed alternative biopsy schedules, belonging to a class of schedules called personalized schedules. Personalized schedules are tailored separately for every patient and every disease. A simple example is the PRIAS schedule, which is personalized since it depends on the PSA-DT of the patient, an indicator of the state of disease. More sophisticated personalized schedules have been developed in the past. For e.g. Bebu and Lachin, 2017 have proposed Markov models based cost optimized personalized schedules. O'Mahony et al., 2015 have proposed cost optimized personalized equi-spaced screening intervals, using Microsimulation Screening Analysis (MISCAN) models. Parmigiani, 1998 have used information theory to come up with schedules for detecting time to event in the smallest possible time interval. Most of these methods however create an entire schedule in advance. Rizopoulos et al., 2016 have proposed dynamic personalized schedules for longitudinal markers using joint models for time to event and longitudinal data(Rizopoulos, 2012; Tsiatis and Davidian, 2004).

The personalized schedules we have proposed in this paper, utilize joint models and are dynamic. i.e. at a time only one future visit is scheduled, based on all the information gathered up to that point in time. More specifically, we have proposed two types of personalized schedules. One based on expected time of GR of a patient and the second based on the risk of GR. We have also analyzed an approach where the two types of personalized schedules are combined. Both types of schedules not only consider a patient's measurable attributes such as age, but also latent patient to patient variations in health, which cannot be measured directly. Results from previous repeat biopsies of the patient and PSA measurements as well as the population level information about hazard of GR, are used by the personalized schedules that we have proposed. It is important to note that a schedule for DRE measurements is not of interest since it is a non invasive procedure and has no serious medical implications. Thus the only event of interest is GR and not disease progression or DRE crossing the threshold of cT2c.

Using joint models to model the PSA measurements and risk of GR has the advantage that the association between the two is also modeled. More importantly, the association is modeled via random effects, and therefore the models have an inherent patient specific nature. Secondly,

joint models allow modeling the entire longitudinal history of PSA measurements, which is more sophisticated than PSA-DT. The use of PSA measurements in creating a personalized schedule is important because PSA is easy to measure, is cost effective and does not have any side effects. Secondly, in PRIAS Bokhorst et al., 2015 found that compliance rate for PSA measurements was as high as 91%. They also showed that there were more men who had a Gleason score greater than 6 as well as PSA-DT less than 3 years compared to men who had Gleason > 6 as well as PSA-DT larger than 3 years. i.e. Information from PSA was found to be indicative of GR. Lastly, some patients/doctors in PRIAS did not comply with the biopsy schedule because they considered PSA to be stable. However, if information from PSA is used in a methodical manner, it can lead to a more informative medical decision making process.

The rest of the paper is organized as follows. Section 2 covers briefly the joint modeling framework in context of the problem at hand. Section 3 details the personalized scheduling approaches we have proposed in this paper. In Section 4 we demonstrate personalized schedules in a real world scenario by employing them for the patients from the PRIAS study. Lastly, in Section 5, we present the results from a simulation study we conducted, to compare personalized schedules with the schedule of PRIAS study, as well with the most aggressive biopsy schedule of doing annual biopsies.

2 Joint models for time to event and longitudinal outcomes

The first step in creating a personalized schedule for biopsies is to come up with a model for Gleason scores, PSA levels and other patient specific characteristics. In PRIAS, PSA levels are measured at the time of induction, every 3 months for the first 2 years in the study and then every 6 months thereafter. Thus PSA levels can be modeled as a longitudinal outcome. As mentioned earlier, patients in PRIAS have a Gleason score of 6 or less at the time of induction in the study, and patients are removed from AS the first time GR takes place. Since our interest lies in finding the time of GR, we model it as a time to event outcome. To model the association between the two types of outcomes we use a joint model for time to event and longitudinal outcomes.

2.1 Joint model specification

Let T_i^* denote the true GR time for the ith patient enrolled in an AS program. Let the vector of times at which a total of g_i biopsies are conducted for the ith patient be denoted by $C_i = \{C_{i0}, C_{i1}, ...C_{ig_i}; C_{ij} < C_{ik}, \forall j < k\}$. T_i^* cannot be observed directly and it is only known that it falls in an interval $(l_i, r_i]$, where $l_i = C_{i(g_i-1)}, r_i = C_{ig_i}$ if GR is observed, and $l_i = C_{ig_i}, r_i = \infty$ if patient drops out of AS. The latter is also known as right censoring. Let $\boldsymbol{y}_i$ denote the $n_i \times 1$ longitudinal outcome vector for the PSA levels of the ith patient. The population of interest consists of all the patients enrolled in AS. For a sample of n patients from this population the observed data is denoted by $\mathcal{D}_n = \{l_i, r_i, \boldsymbol{y}_i; i = 1, \ldots n\}$.

To model the evolution of the PSA measurements over time, the joint model utilizes a linear mixed effects model. The longitudinal outcome $y_i(t)$ at a time t is modeled as:

$$y_i(t) = m_i(t) + \varepsilon_i(t),$$
$$= \boldsymbol{x}_i^T(t)\boldsymbol{\beta} + \boldsymbol{z}_i^T(t)\boldsymbol{b}_i + \varepsilon_i(t)$$

where, $m_i(t)$ denotes the true and unobserved value of the longitudinal outcome at time t. The measurement error $\varepsilon_i(t) \sim N(0, \sigma^2)$ is assumed normally distributed with variance σ^2. $\boldsymbol{\beta}$ denotes the vector of the unknown fixed-effects parameters. $\boldsymbol{b}_i \sim N(0, \boldsymbol{D})$ denotes the $q \times 1$ vector of random effects, assumed normally distributed with mean zero, and $q \times q$ covariance matrix $\boldsymbol{D}$. $\boldsymbol{b}_i$ and $\varepsilon_i(t)$ are assumed independent. $\boldsymbol{x}_i(t)$ and $\boldsymbol{z}_i(t)$ denote row vectors of the design matrices for the fixed and random effects, respectively. For non continuous longitudinal outcomes, joint models utilize Generalized linear mixed models (Rizopoulos, 2012).

To model the effect of PSA measurements on risk of GR, joint models utilize a relative risk sub-model where the hazard of GR at any time point t, denoted by $h_i(t)$, depends on the history of true

and unobserved values of PSA levels $\mathcal{M}_i(t) = \{m_i(v), 0 \leq v \leq t\}$ measured up to that time point. Joint models offer flexibility in modeling this dependence. In its simplest form, the hazard may depend on instantaneous value of PSA $m_i(t)$ at time t. More sophisticated ones are dependence of hazard at time t on PSA-DT, PSA velocity $m_i'(t) = \dfrac{dm_i(t)}{dt}$, or even on the cumulative effect of PSA $\int_0^t m_i(s)\, ds$ up to t. The fact that any functional form of dependence is possible, is evident from the following expression for hazard at time t:

$$h_i(t \mid M_i(t), \boldsymbol{w}_i) = h_0(t)\exp[\boldsymbol{\gamma}^T \boldsymbol{w}_i + f\{M_i(t), \boldsymbol{b}_i, \boldsymbol{\alpha}\}]$$

where $h_0(t)$ is the baseline hazard at time t. $\boldsymbol{w}_i$ is a vector of baseline covariates and $\boldsymbol{\gamma}$ are the corresponding parameters. The function $f(\cdot)$ parametrized by vector $\boldsymbol{\alpha}$ specifies the function form of longitudinal outcome that is used in the linear predictor of the relative risk model.

While $\boldsymbol{\alpha}$ controls the strength of association between the hazard of GR and features of the PSA history, the fact that both Gleason scores and PSA levels are internally related to a patient's health, is manifested by the random effects $\boldsymbol{b}_i$ in the model. The joint model postulates that given the random effects, time to GR and the different PSA measurements taken over time are all mutually independent. As mentioned earlier, in PRIAS study PSA-DT is used to decide the schedule of biopsies. Although PSA-DT is computed using observed PSA values, dependence on observed longitudinal history $\mathcal{Y}(t) = \{y_i(v), 0 \leq v \leq t\}$ at any time t, is not the same as dependence on patient's health. On the contrary dependence on patient's health, manifested by $\boldsymbol{b}_i$ is same as dependence on future unobserved values of PSA. Thus the inference for the model parameters $\boldsymbol{\theta} = \{\boldsymbol{\beta}^T, \boldsymbol{\gamma}^T, \boldsymbol{\alpha}^T, \sigma^2, \{d_{jk} \mid j = k = 1, ...q\}\}^T$ doesn't change even if uncertainty in biopsy schedule C_i is not modeled. The kernel of the corresponding joint likelihood conditional on the random effects and the model parameters is given by:

$$p(T_i, l_i, r_i, \boldsymbol{y}_i \mid \boldsymbol{b}_i, \boldsymbol{\theta}) \propto p(T_i \mid l_i, r_i, \boldsymbol{b}_i, \boldsymbol{\theta})p(\boldsymbol{y}_i \mid \boldsymbol{b}_i, \boldsymbol{\theta})$$

3 Personalized schedules for repeat biopsies

Once a joint model for GR and PSA levels is obtained, the next step is to use it to create personalized schedules for biopsies. To elucidate the scheduling methods, let us assume that the a personalized schedule is to be created a new patient enumerated j, who is not present in the original sample of patients $\mathcal{D}_n$. Further let us assume that this patient did not have a GR at their last biopsy performed at time t, and that the PSA measurements are available up to a time point s. The goal is to find the optimal time $u \geq \max(t, s)$ of the next biopsy each time results from repeat biopsy or a PSA measurement is available.

3.1 Posterior predictive distribution for time to GR

Let $\mathcal{Y}_j(s)$ denote the history of PSA measurements taken up to time s for patient j. The information from PSA history and repeat biopsies is manifested by the posterior predictive distribution $g(T_j^*)$. It is given by (conditioning on baseline covariates $\boldsymbol{w}_i$ is dropped for notational simplicity here onwards):

$$\begin{aligned}
g(T_j^*) &= p(T_j^* \mid T_j^* > t, \mathcal{Y}_j(s), \mathcal{D}_n) \\
&= \int p(T_j^* \mid T_j^* > t, \mathcal{Y}_j(s), \boldsymbol{\theta})p(\boldsymbol{\theta} \mid \mathcal{D}_n)\, d\boldsymbol{\theta} \\
&= \int \int p(T_j^* \mid T_j^* > t, \boldsymbol{b_j}, \boldsymbol{\theta})p(\boldsymbol{b}_j \mid T_j^* > t, \mathcal{Y}_j(s), \boldsymbol{\theta})p(\boldsymbol{\theta} \mid \mathcal{D}_n)\, d\boldsymbol{b}_j\, d\boldsymbol{\theta}
\end{aligned} \tag{1}$$

The posterior predictive distribution depends on the observed longitudinal history via the random effects $\boldsymbol{b_j}$. The posterior distribution of the parameters $\boldsymbol{\theta}$, denoted by $p(\boldsymbol{\theta} \mid \mathcal{D}_n)$ is obtained from the joint model fitted to the original data set of patients $\mathcal{D}_n$.

3.2 Loss functions

To find the time u of next biopsy, we use principles from statistical decision theory in a Bayesian setting (Berger, 1985; Robert, 2007). More specifically, we propose to choose future biopsy time u by minimizing the posterior expected loss $E_g[L(T_j^*, u)]$, where the expectation is taken w.r.t. the posterior predictive distribution $g(T_j^*)$.

$$E_g[L(T_j^*, u)] = \int_t^\infty L(T_j^*, u) p(T_j^* \mid T_j^* > t, \mathcal{Y}_j(s), \mathcal{D}_n) \, dT_j^*$$

Various loss functions $L(T_j^*, u)$ have been proposed in literature (Robert, 2007). The ones we utilize, and the corresponding motivations are presented next.

3.2.1 Expected and median time of GR

One of the reasons, patients did not comply with the existing PRIAS schedule was 'complications on a previous biopsy'. Therefore, it makes sense to have as less biopsies as possible. In the ideal case only 1 biopsy, performed at the exact time of GR is sufficient. Hence, neither a time which overshoots the true GR time T_j^*, nor a time which undershoots is preferred. In this regard, the squared loss function $L(T_j^*, u) = (T_j^* - u)^2$ and absolute loss function $L(T_j^*, u) = \mid T_j^* - u \mid$ have the properties that the posterior expected loss is symmetric on both sides of T_j^*. Secondly, both loss functions have well known solutions available. The posterior expected loss for the squared loss function is given by:

$$\begin{aligned} E_g[L(T_j^*, u)] &= E_g[(T_j^* - u)^2] \\ &= E_g[(T_j^*)^2] + u^2 - 2u E_g[T_j^*] \end{aligned} \tag{2}$$

The posterior expected loss in equation (2) attains its minimum at $u = E_g[T_j^*]$, also known as expected time of GR. The posterior expected loss for the absolute loss function is given by:

$$\begin{aligned} E_g[L(T_j^*, u)] &= E_g[\mid T_j^* - u \mid] \\ &= \int_u^\infty (T_j^* - u) g(T_j^*) \, dT_j^* + \int_t^u (u - T_j^*) g(T_j^*) \, dT_j^* \end{aligned} \tag{3}$$

The posterior absolute loss in equation (3) attains its minimum at the median of $g(T_j^*)$, given by $u = \pi^{-1}(0.5)$, where $\pi^{-1}(\cdot)$ is the inverse of dynamic survival probability $\pi_j(u \mid t, s)$ of patient j (Rizopoulos, 2011). It is given by:

$$\pi_j(u \mid t, s) = Pr(T_j^* \geq u \mid T_j^* > t, \mathcal{Y}_j(s), D_n), u \geq t \tag{4}$$

3.2.2 Dynamic risk of GR

In a practical scenario it is possible that a doctor or a patient may not want to exceed a certain risk of GR $1 - \pi_j(u \mid t, s)$ since the last biopsy. This may be also useful in the cases where variance of $g(T_j^*)$ is high, rendering expected time of GR, or any other measure of central tendency of $g(T_j^*)$ unsuitable. The personalized scheduling approach based on dynamic risk of GR, schedules the next biopsy at a time point u such that the dynamic risk of GR is higher than a certain threshold $1 - \kappa$, $\kappa \epsilon [0, 1]$ beyond u. Or in other words the dynamic survival probability $\pi_j(u \mid t, s)$ is below a threshold κ beyond u. To this end, the posterior expected loss for the following multilinear loss function can be minimized to find the optimal u:

$$L_{k_1, k_2}(T_j^*, u) = \begin{cases} k_2(T_j^* - u) & if(T_j^* > u) \\ k_1(u - T_j^*) & \text{otherwise} \end{cases} \tag{5}$$

where $k_1 > 0$, $k_2 > 0$ are constants parameterizing the loss function. The posterior expected loss function $E_g[L_{k_1, k_2}(T_j^*, u)]$ obtains its minimum at $u = \pi_j^{-1}\left\{ \dfrac{k_1}{k_1 + k_2} \right\}$ (Robert, 2007). The choice of k_1, k_2 is equivalent to the choice of κ. More specifically, $\kappa = \dfrac{k_1}{k_1 + k_2}$.

3.3 A mixed approach between $E_g[T_j^*]$ and dynamic risk of GR

When the variance $Var_g[T_j^*]$ of $g(T_j^*)$ is small, then $E_g[T_j^*]$ is practically very useful. However when the variance is large, there may not be a clear central tendency of the distribution and $E_g[T_j^*]$ will either overshoot T_j^* or undershoot it by a big margin. In the latter case more biopsies will be required until GR is detected at some time point $T_{jN_j^b} > T_j^*$. The overshooting margin can be measured as an offset $O_j = T_{jN_j^b} - T_j^*$. The maximum acceptable O_j in PRIAS is 3 years, which corresponds to the time gap between biopsies of the PRIAS fixed schedule. When $Var_g[T_j^*]$ is large, the proposals based on $E_g[T_j^*]$ can have a large O_j. Thus we propose that if the difference between the 0.025 quantile and $E_g[T_j^*]$ is more than 3 years then proposals based on dynamic risk of GR be used instead. We call this approach a mixed approach.

3.4 Estimation

3.4.1 Estimation of $E_g[T_j^*]$ and $Var_g[T_j^*]$

Since there is no closed form solution available for $E_g[T_j^*]$, for its estimation we utilize the following relationship between expected time of GR and dynamic survival probability:

$$E_g[T_j^*] = t + \int_t^\infty \pi_j(u \mid t, s)\, du$$

There is no closed form solution available for the integral and hence we approximate it using Gauss-Kronrod quadrature. We preferred this approach over Monte Carlo methods to estimate $E_g[T_j^*]$ from the posterior predictive distribution $g(T_j^*)$. This was done because sampling directly from $g(T_j^*)$ involved an additional step of sampling from the distribution $p(T_j^* \mid T_j^* > t, \boldsymbol{b_j}, \boldsymbol{\theta})$, as compared to the estimation of $\pi_j(u \mid t, s)$ (Rizopoulos, 2011). Thus the latter approach was computationally faster. As mentioned earlier, a limitation of expected time of GR is that it is practically useful only when the variance of predictive distribution $g(T_j^*)$ is small. The variance is given by:

$$Var_g[T_j^*] = E_g[T_j^{*2}] - E_g[T_j^*]^2$$
$$= 2\int_t^\infty (u-t)\pi_j(u \mid t, s)\, du - \left(\int_t^\infty \pi_j(u \mid t, s)\, du \right)^2 \tag{6}$$

Since a closed form solution is not available for the variance expression, it is estimated similar to the estimation of $E_g[T_j^*]$. The variance depends both on last biopsy time t and PSA history $\mathcal{Y}_j(s)$. The impact of the observed information on variance is detailed in Section 4.2.

3.4.2 Estimation of κ

For schedules based on dynamic risk of GR, the value of κ dictates the biopsy schedule and thus its choice has important consequences. In certain cases it may be chosen on the basis of doctor's advice or the amount of risk that is acceptable to the patient. For e.g. if maximum acceptable risk is 75% then $\kappa = 0.25$, and correspondingly all $k_1, k_2 \mid k_1 = \dfrac{k_2}{3}$ can be used in equation (5) to calculate u.

While a doctor's advice can be invaluable, it is also possible to automate the choice of κ. We propose to choose a κ for which a binary classification accuracy measure (López-Ratón et al., 2014; Sokolova and Lapalme, 2009), discriminating between cases and controls, is maximized. In PRIAS, cases are patients who experience GR and the rest are controls. However, a patient can be in control group at some time t_a and in the cases at some future time point $t_b > t_a$, and thus time dependent binary classification is more relevant. In joint models, a patient j is predicted to be a case if $\pi_j(t + \Delta t \mid t, s) \leq \kappa$ and a control if $\pi_j(t + \Delta t \mid t, s) > \kappa$ (Rizopoulos, 2014). The time window Δt can be either chosen on a clinical basis, or such that uncertainty in estimation of $\pi_j(t + \Delta t \mid t, s)$ is below a certain threshold or it can even be chosen such that $AUC(t, \Delta t, s)$ (Rizopoulos, 2014) is largest. i.e. Δt for which the model has the most discriminative capability at time t. The binary classification accuracy measures we maximize to select the threshold κ are

the following (the binary classification measures are functions of $t, \Delta t, s$, however the notation is dropped for readability):

- Accuracy: $ACC = \dfrac{TP + TN}{TP + FP + TN + FN}$, where TP, FP, TN and FN are the number of true positives, false positives, true negatives and false negatives at time point t. In this case if $k_1 = TP + TN$ and $k_2 = FP + FN$, then $\underset{k_1, k_2}{\arg \max} \ ACC$ gives the optimal k_1, k_2 or equivalently the κ.

- Youden's index: $J = \text{Sensitivity} + \text{Specificity} - 1$,
  where sensitivity is defined as $Pr(\pi_j(t + \Delta t \mid t, s) \leq \kappa \mid T_j^* \epsilon(t, t + \Delta t])$ and specificity is defined as $Pr(\pi_j(t + \Delta t \mid t, s) > \kappa \mid T_j^* > t + \Delta t)$ (Rizopoulos, 2014). In this case if $k_1 = FP \cdot TP - FN \cdot TN$ and $k_2 = (TP + FN)(FP + TN) - k_1$, then $\underset{k_1, k_2}{\arg \max} \ J$ gives the optimal k_1, k_2 or equivalently the κ.

- F1 Score: $F1 = \dfrac{2TP}{2TP + FP + FN}$. In this case if $k_1 = 2TP$ and $k_2 = FP + FN$, then $\underset{k_1, k_2}{\arg \max} \ F1$ gives the optimal k_1, k_2 or equivalently the κ.

3.5 Algorithm

The algorithm in Figure 1 elucidates the process of creating a personalized schedule for patient j. In the algorithm:

1. t denotes the time of the latest biopsy.

2. s denotes the time of the latest available PSA measurement.

3. u denotes the personalized biopsy time based on $g(T_j^*)$.

4. u^{pv} denotes the time at which a repeat biopsy was proposed at the last visit to the hospital.

5. T^{nv} denotes the time of the next visit for PSA measurement.

Since PRIAS and most AS programs strongly advise against conducting more than 1 biopsy per year, the algorithm adjusts the optimal time u of biopsy in case the last biopsy was within an year.

4 Personalized schedules for patients in PRIAS

To demonstrate how the personalized scheduling algorithm described in Section **??** works, we apply it to the patients in the PRIAS dataset. To this end, we divide the PRIAS data set into training(5264 patients) and demonstration data sets (3 patients). We fit a joint model to the training data set and then use it to create a personalized schedule for patients in demonstration data set. We fit the joint model using the R package JMbayes (Rizopoulos, 2014), which uses the Bayesian methodology to estimate the model parameters.

4.1 Fitting the joint model to PRIAS dataset

The training data set contains information about 5938 prostate cancer patients who satisfied the conditions for enrollment in AS. For every patient the age at the time of induction in AS was recorded. PSA was measured every 3 months for first 2 years and every 6 months thereafter. To detect GR, biopsies were conducted at different time points on the basis of a predetermined schedule as well as PSA-DT as described in Section 1. For the longitudinal analysis of PSA measurements we used $\log_2 PSA$ measurements instead of the raw data. The log transformation was done because the PSA scores took very large values around the time of disease progression. This indicated that the underlying distribution for PSA scores was right skewed. The longitudinal sub-model of the joint model we fit is given by:
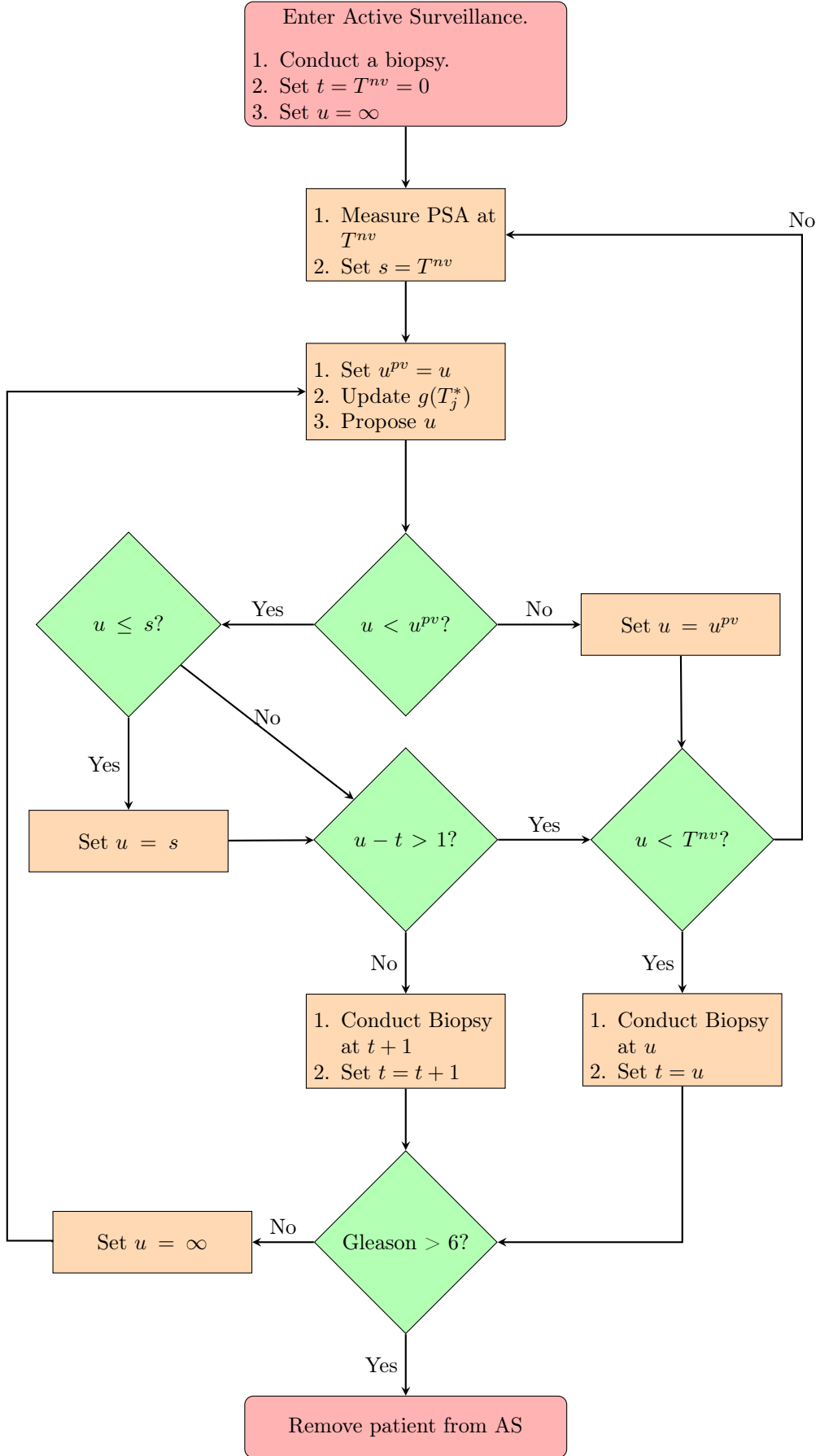
Figure 1: Algorithm for creating a personalized schedule for patient j.

$$\log_2 PSA(t) = m_i(t) + \varepsilon_i(t),$$
$$m_i(t) = (\beta_0 + b_{i0}) + \beta_1(Age - 70) + \beta_2(Age - 70)^2$$
$$+ \sum_{k=1}^{4} \beta_{k+2} B_k(t, \mathcal{K}) + b_{i1} B_7(t, 0.5) + b_{i2} B_8(t, 0.5)$$
$$\varepsilon_i(t) \sim N(0, \sigma^2),$$
$$\boldsymbol{b}_i \sim N(0, \boldsymbol{D})$$

The evolution of PSA levels over time is modeled flexibly using B-splines. For the fixed effects part the spline consists of 3 internal knots. The internal knots are at $\mathcal{K} = \{0.5, 1.2, 2.5\}$ years, and boundary knots are at 0 and 7 years. For the random effects part there is only 1 internal knot at 0.5 years and the boundary knots are at 0 and 7 years. The choice of knots was based on exploratory analysis as well as on the basis of model selection criteria AIC and BIC. The variable Age was median centered to avoid numerical instabilities while estimating the parameters in the model. For the survival sub-model the hazard function we fitted is given by:

$$h_i(t) = h_0(t) \exp[\gamma_1(Age - 70) + \gamma_2(Age - 70)^2 \alpha_1 m_i(t) + \alpha_2 m_i'(t)] \tag{7}$$

where, α_1 and α_2 are measures of strength of association between hazard of GR and PSA value $m_i(t)$ and PSA velocity $m_i'(t)$, respectively. $h_0(t)$ is the baseline hazard at time t, and is modeled flexibly using P-splines(Eilers and Marx, 1996). Lastly, to fit the joint model we use the R package JMbayes Rizopoulos, 2014, which uses a Bayesian approach for parameter estimation.

4.1.1 Parameter Estimates

The posterior parameter estimates $p(\boldsymbol{\theta} \mid \mathcal{D}^{PRIAS})$ for the joint model we fitted to the PRIAS data set are shown in Table 1 and Table 2. Since the longitudinal evolution of $\log_2 PSA$ is modeled with non-linear terms, the interpretation of the coefficients corresponding to time is not straightforward. In lieu of the interpretation we present the fitted evolution of PSA over a period of 10 years for a patient who is 70 years old in Figure 2. It can be seen that the after the first 6 months the PSA levels steadily increase over the follow up period. Since the model for PSA has only additive terms, this evolution remains same for all patients. The effect of Age only affects the baseline PSA score. However it is so small that it can be ignored for all practical purposes.

	Mean	Std. Dev	2.5%	97.5%	P
Intercept	2.455	0.012	2.433	2.480	<0.000
(Age - 70)	0.003	0.001	4.9×10^{-4}	0.006	0.032
(Age - 70) × (Age - 70)	-0.001	1.4×10^{-4}	-0.001	-3.5×10^{-4}	<0.000
Spline: visitTimeYears[0, 0.5]	-0.006	0.012	-0.031	0.017	0.674
Spline: visitTimeYears[0.5, 1.2]	0.228	0.019	0.192	0.265	<0.000
Spline: visitTimeYears[1.2, 2.5]	0.140	0.029	0.088	0.197	<0.000
Spline: visitTimeYears[2.5, 7]	0.303	0.039	0.227	0.379	<0.000
σ	0.324	0.001	0.321	0.326	

Table 1: Longitudinal sub-model estimates for joint model.

For the survival sub-model, the parameter estimates in Table 2 show that only $\log_2 PSA$ velocity is strongly associated with hazard of GR. For any patient, a unit increase in $\log_2 PSA$ velocity corresponds to a 11 time increase in hazard of GR. The effect of $\log_2 PSA$ value and effect of Age on hazard of GR are so small that they can be safely ignored for all practical purposes.

4.2 Demonstration of personalized schedules

In this section, we demonstrate how the personalized scheduling algorithm adapts the time of performing a biopsy according to the PSA history and results from repeat biopsies. The 3 patients we have chosen for the demonstration data set are part of PRIAS program and they have had
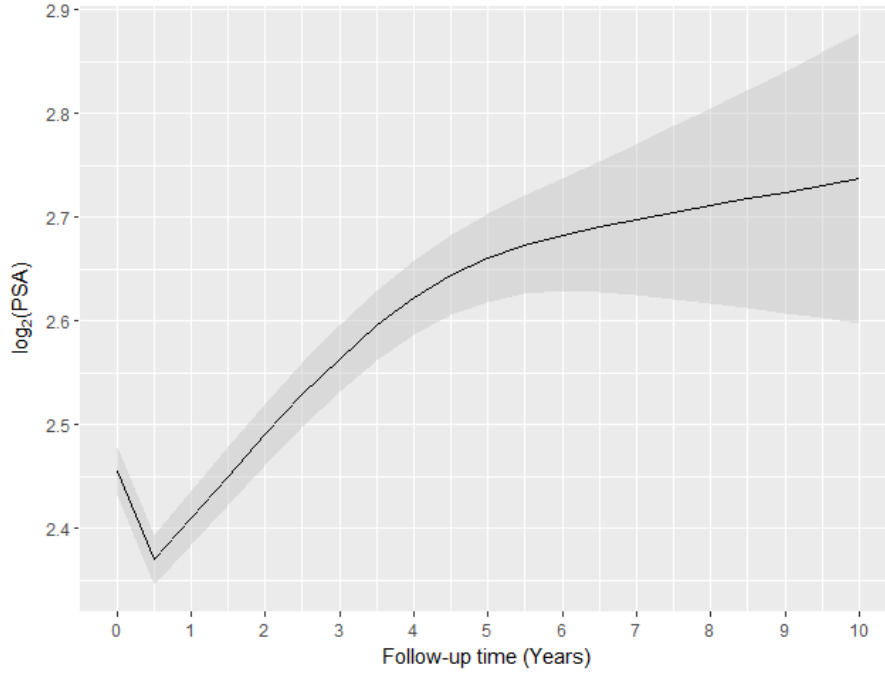
Figure 2: Fitted evolution of $\log_2 PSA$ over a period of 10 years, for a patient who was inducted in AS at the Age of 70 years.

Variable	Mean	Std. Dev	2.5%	97.5%	P
Age - 70	0.037	0.006	0.025	0.0490	<0.000
(Age - 70) $\times$ (Age - 70)	-0.001	0.001	-0.003	1.8×10^{-4}	0.104
$\log_2 PSA$	-0.049	0.064	-0.172	0.078	0.414
Slope: $\log_2 PSA$	2.407	0.319	1.791	3.069	<0.000

Table 2: Survival sub-model estimates for joint model.

their repeat biopsies already. Hence a full scale comparison between PRIAS biopsy schedule and personalized scheduling algorithm's biopsy schedule is not possible.

The first patient of interest is patient nr. 3174 who was inducted in the PRIAS program at the age of 74 years. Between the last follow up and time of induction there was no repeat biopsy performed for this patient. Hence the predictive distribution $g(T_j^*)$ for this patient depends only on the PSA measurements. For this patient, the evolution of PSA, time of last biopsy and proposed times of biopsies are shown in Figure 3. It can be seen that the PSA remains stable for the first 2 years of follow ups, but increases rapidly after that for the next 2 years of follow up. Since the hazard of GR depends on PSA velocity (Table2), the schedule of biopsy based on personalized scheduling algorithm (Section 1), adjust the times of biopsy according to the steep rise in PSA profile. At 2 years the expected and median time of GR are 12.5 years and 15.2 years respectively, whereas at 4 years, they are 5.3 and 4 years respectively. It is important to note that the estimates are year 2 are not as useful as the estimates at year 4, because the $Var_g[T_j^*]$ is considerably lower at year 4, as shown in Figure ??.

The second patient of interest is patient nr. 911. Figure 4 shows the evolution of PSA, time of last biopsy and proposed biopsy times for this patient. Firstly, it can be seen that at between year 1.5 and year 2, the PSA rises sharply, and accordingly the personalized schedules based on expected time of GR preponed the proposed biopsy time from 14.2 years to 13.8 years. The change in median time of GR is trivial. The second observation is that between year 2 and year 3 the PSA decreases sharply and accordingly, the proposed biopsy times are postponed. More specifically the median time of GR increased from 15.2 years at year 2 to 17 years at year 3. Whereas the expected time of GR increased from 13.8 years to 16.6 years. It can also be seen that PSA remains stable
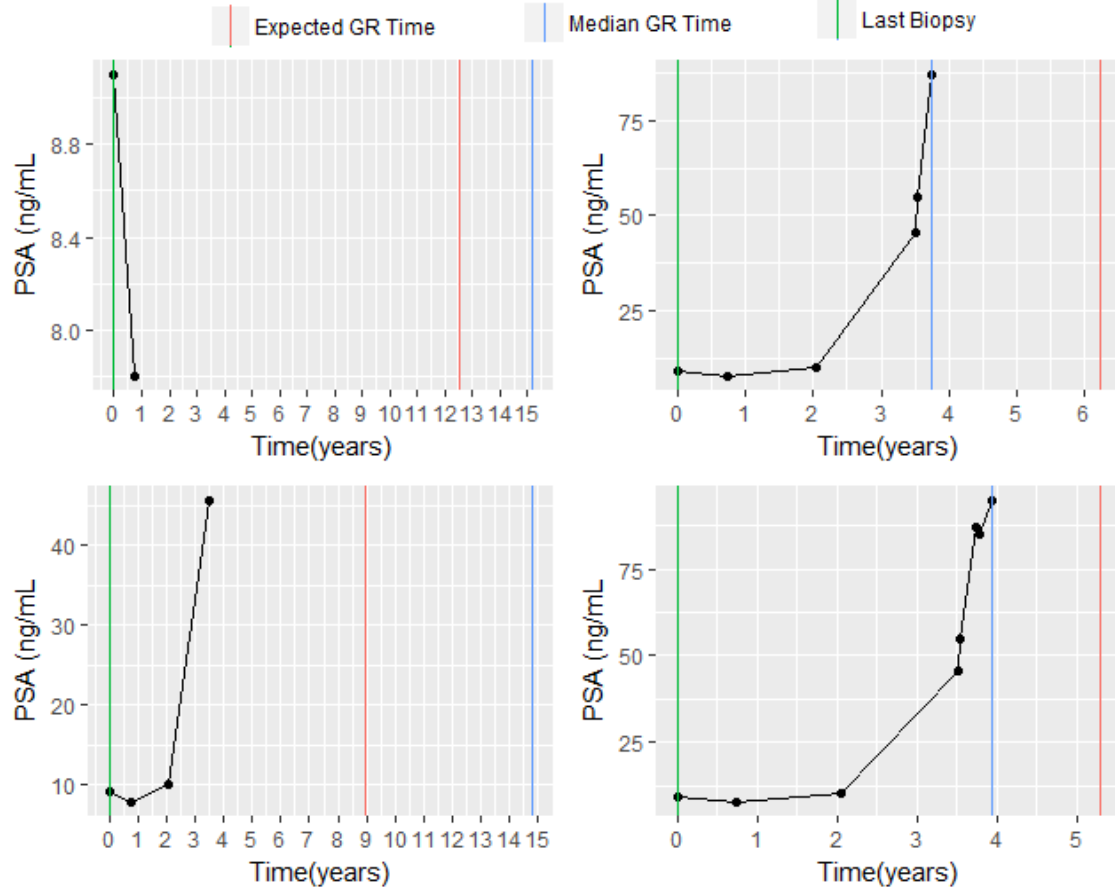
Figure 3: Proposed biopsy times for patient 3174 from PRIAS.

up to to year 4. Lastly, because no GR is found at the repeat biopsy performed at 4.1 years, this further leads to postponing of the biopsy times, which become 18.7 and 19.9 for expected time of GR and median time of GR respectively.

The fact that PSA velocity affects the biopsy times is also evident in the case of patient 2340, whose PSA evolution is shown in Figure 5. We have purposefully ignored all the biopsies conducted for this patient in PRIAS, to isolate the effect of PSA history. It can be seen that PSA slowly rises to a value of 14 ng/mL over a period of 2.5 years. Correspondingly, there is little change in proposed biopsy times. On the other hand between 2.3 years and 3.3 years the PSA rises very sharply and correspondingly the expected time of GR decreases by an year from 12.5 years to 11.5 years in that period. The median time of GR remains the same though.

5   Simulation study

The application of personalized schedules for patients in PRIAS demonstrated that personalized schedules adapt according to the history of each patient. However, since the patients in PRIAS have already had their biopsies as per the PRIAS schedule, we were not able to evaluate the efficacy of personalized schedules against the PRIAS schedule. To this end, we have performed a simulation study to compare 3 broad categories of schedules: Personalized schedules, PRIAS schedule and a schedule of annual biopsy.

5.1   Simulation setup

In the simulation study we used a total of 100 data sets with 1000 patients each. For each of the patients in the 100 data sets, we generated the longitudinal profiles using the posterior estimates of the parameters $p(\boldsymbol{\theta} \mid \mathcal{D}^{PRIAS})$ from the joint model fitted to the PRIAS data set (Section 4.1).
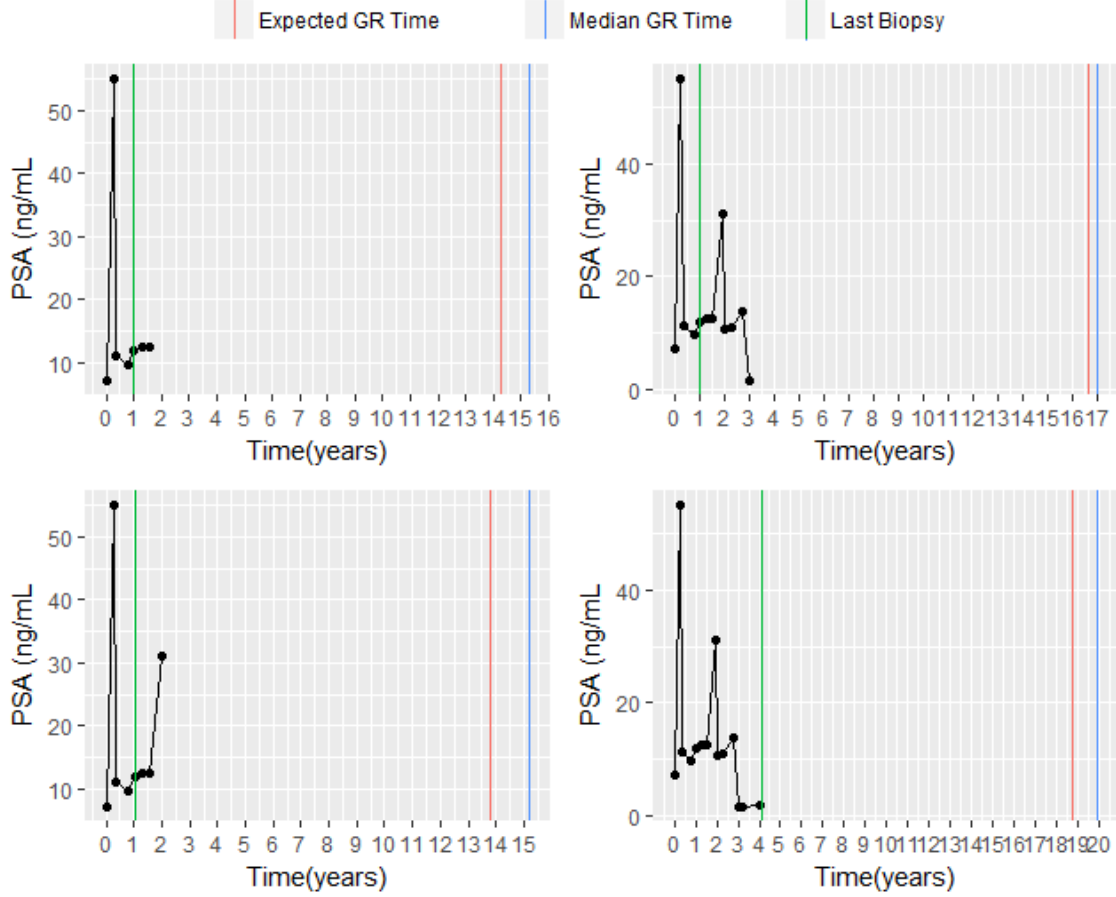
Figure 4: Proposed biopsy times for patient 911 from PRIAS.

The visit times for PSA measurements were the same as PRIAS schedule. i.e. Every 3 months for first 2 years and every 6 months thereafter. Similarly, while generating Gleason reclassification times for the patients, the parameters of the linear predictor in the hazard function (Equation 7) were obtained from the joint model fitted to PRIAS data set. However unlike the flexibly modeled baseline hazard in PRIAS joint model, the baseline hazard in the simulation study was modeled using a Weibull distribution. We used 10 sets of parameters $\Omega_g = \{\lambda_g, k_g\}; g = 1, ...10$ for the Weibull baseline hazard, one each for a group g of 10 data sets. This was done, firstly to ensure that different data sets $\mathcal{D}_k^g; k = 1, ...10$ within a group are sampled from the same population $\mathcal{P}_g$ of patients. This way we could isolate the variation in the performance of a scheduling method. Secondly, different parameter values for the baseline hazard across the groups ensured that we tested different patient populations; those who have early progression times, as well as those who have late progression times. This is important because how late or early patients are observed to have GR, partly depends on the induction criteria of the AS program. (**Give the values of Ω for different populations and the corresponding histograms of GR times.**)

In a real life scenario the parameters $\boldsymbol{\theta}$ of a joint model for hazard of GR and PSA measurements will not be known in advance, and hence we do not use posterior estimates $p(\boldsymbol{\theta} \mid \mathcal{D}^{PRIAS})$ from the joint model fitted to the PRIAS data set to create personalized schedule for the simulated patients. Instead we divide each of the 100 simulated data sets into training (750 patients) and test (250 patients) parts. For ease of notation we reuse $\mathcal{D}_k^g$ as the notation for the kth training data set from the gth group. Further we simulate random and non-informative censoring times for the patients in training data set. Thus $\mathcal{D}_k^g = \{T_i, \delta_i, \boldsymbol{y}_i; i = 1, ...750\}$. $T_i = \min(T_i, C_i)$ denotes the observed GR time for the ith patient in training data set. $\delta_i = I(T_i < C_i)$ is the event indicator, where $I(\cdot)$ is an indicator function that takes the value 1 when $T_i < C_i$ and 0 otherwise. We then fit a joint model to the training data set to obtain posterior estimates of parameters $p(\boldsymbol{\theta} \mid \mathcal{D}_k^g)$, which are required for the predictive distribution $g(T_j^*)$ of the jth patient from the test data set.
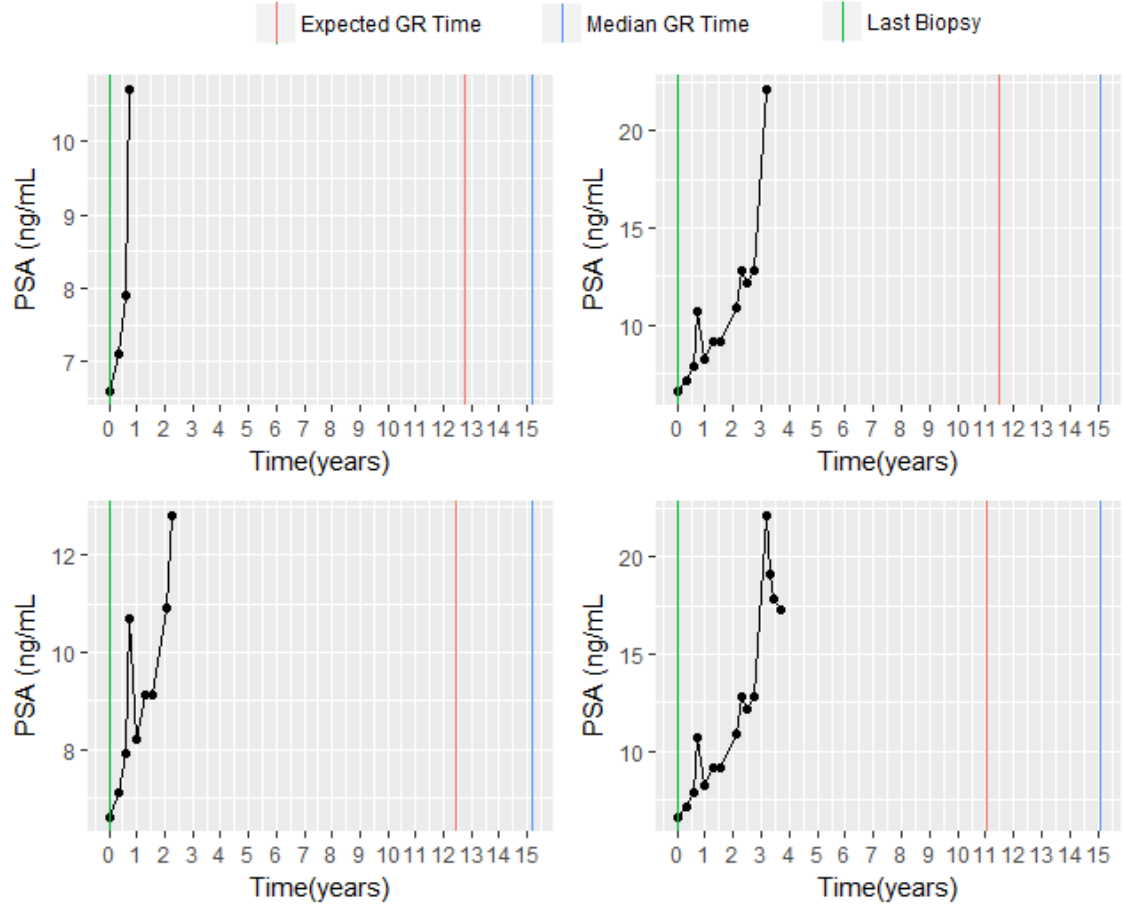
Figure 5: Proposed biopsy times for patient 2340 from PRIAS.

While the predictive distribution is sufficient for scheduling biopsies based on expected time of GR, the choice of time window Δt (Section 3.2.2) has to be made for scheduling biopsies on the basis of dynamic risk of GR. In PRIAS and in most AS programs biopsies are done at a gap of 1 to 3 years. A gap of 1 year between biopsies detects GR the earliest and at maximum detection of GR can be delayed by 1 year. Correspondingly, if we choose a time window Δt of 1 year, then eventually the choice of κ differentiates between people who fail .... Different κ values maximize the binary classification measures [REFER HERE] at different time points. To this end, we first compute the binary classification measures over a fine grid of time points using the training data set, and then obtain the corresponding κ values. For the test patients κ values corresponding to a time point from the grid which is nearest to the last biopsy time of the patient, are used [WRITE IT MATHEMATICALLY?]. Lastly, to create the personalized schedules, we use the algorithm described in Section **??**.

5.2 Evaluating efficacy of scheduling methods

For a given population of patients $\mathcal{P}_g$, the first criteria in evaluation of efficacy of a schedule S for biopsies is the number of repeat biopsies N_g^S it takes before GR is detected for a patient from the population. The less N_g^S the better it is for patients. In case of annual schedule, N_g^S depend only on the true GR time T_g^* of a patient. On the other hand, for PRIAS and personalized schedules N_g^S depend on PSA measurements $\boldsymbol{y}_g$ as well as on true GR time. In either case, the marginal distribution of the number of biopsies $p(N_g^S)$ for the entire population is unknown. We estimate the mean and quantiles of this distribution from the observed number of biopsies $N_{g_{kj}}^S; j = 1, ...250$ for each of the 250 test patients in the kth data set of the gth group (**Should we instead take mean of means using the 10 data sets?**). The second criteria in evaluation of efficacy of a schedule is the offset $O_g^S = T_g^S - T_g^*$, where $T_g^S > T_g^*$ is the time at which GR is detected by the scheduling mechanism S. Once again the marginal distribution $p(O_g^S)$ is not known. We estimate

13

the mean and quantiles of this distribution from the observed offset $O_{g_{k_j}}^S; j = 1,...250$ for each of the 250 test patients in the kth data set of the gth group.

Certain scheduling mechanisms may have a smaller mean offset $E[O_g^S]$, but they may schedule a lot of biopsies. One such schedule is the annual repeat biopsy schedule. No matter what the GR time for a patient is, the offset will never be more than 1 year. The vice versa of this scenario is also possible. Given the medical aspects of biopsies, it is not possible to prefer one criteria over another. For e.g. A doctor may choose a schedule with the least mean number of biopsies possible as long as the mean offset is below a certain threshold; such as 3 years in PRIAS. But certain schedules have a small mean offset $E[O_g^S]$, while simultaneously having a high variance $Var[O_g^S]$. i.e. the scheduling mechanism is not suitable for everyone in the population. In such a case the doctor may put a threshold on offset not being larger than a certain number of months for $p\%$ of the patients. The choice of p can be done on the basis of patient's consent or an AS program's policy.

5.3 Results

Since the Gleason reclassification times varied widely across the simulation data sets, we discuss the results separately for the different scenarios. In total we have 6 scenarios corresponding to the 6 groups of 10 data sets. For brevity, we only chose 3 most dissimilar scenarios and further we present one set of results for each of the 3 scenarios. The complete set of results can be found at https://goo.gl/u6dg8G. At this moment, we will not compare our results against the PRIAS schedule, since the PRIAS schedule we used is fixed for all patients, whereas in reality it can be dynamic if the PSA doubling time is less than 10 years.

5.3.1 Scenario 1

In the first scenario the Gleason reclassification times for the patients are mostly between 7 and 11 years. The Gleason reclassification times of test patients from one of the data sets is shown in Figure 6. Figure 9 shows that, for this data set the approaches with the least number of biopsies, 2 in number, are conditional expected failure time, and dynamic risk with a threshold κ chosen such that accuracy (section 3.2.2) is maximized. The mean and median offset for the two approaches is around 9 months. However for a few outlying patients the offset is more than 24 months. If we compare this to the schedule of performing biopsy every year the mean offset is around 6 months and mean number of biopsies is 8.
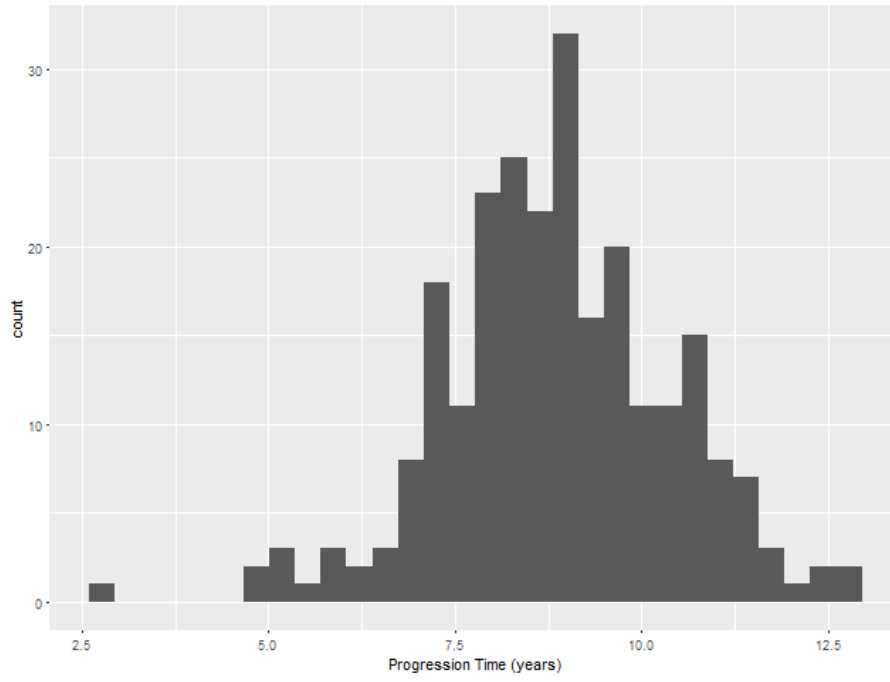
Figure 6: Gleason reclassification times for patients from the test data set of scenario 1.
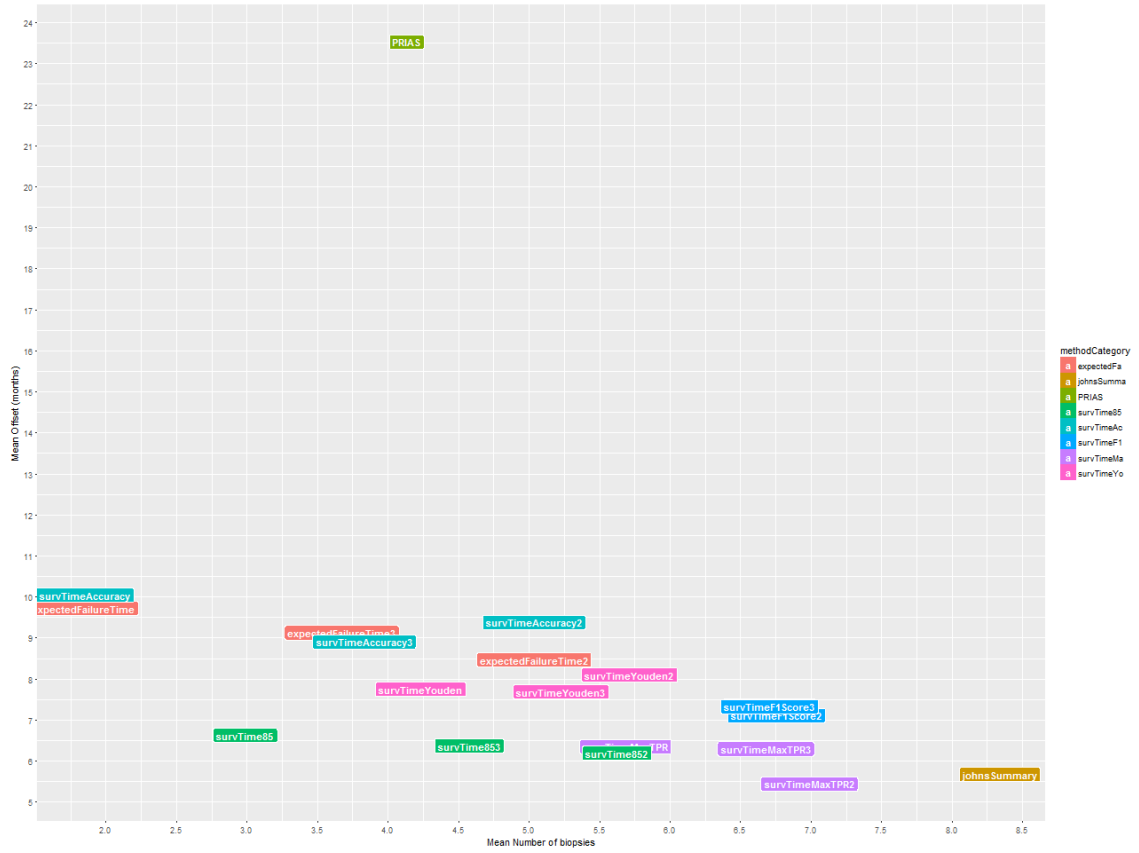

Figure 7: Mean number of biopsies against the mean offset (in years) for each of the approaches in scenario 1.
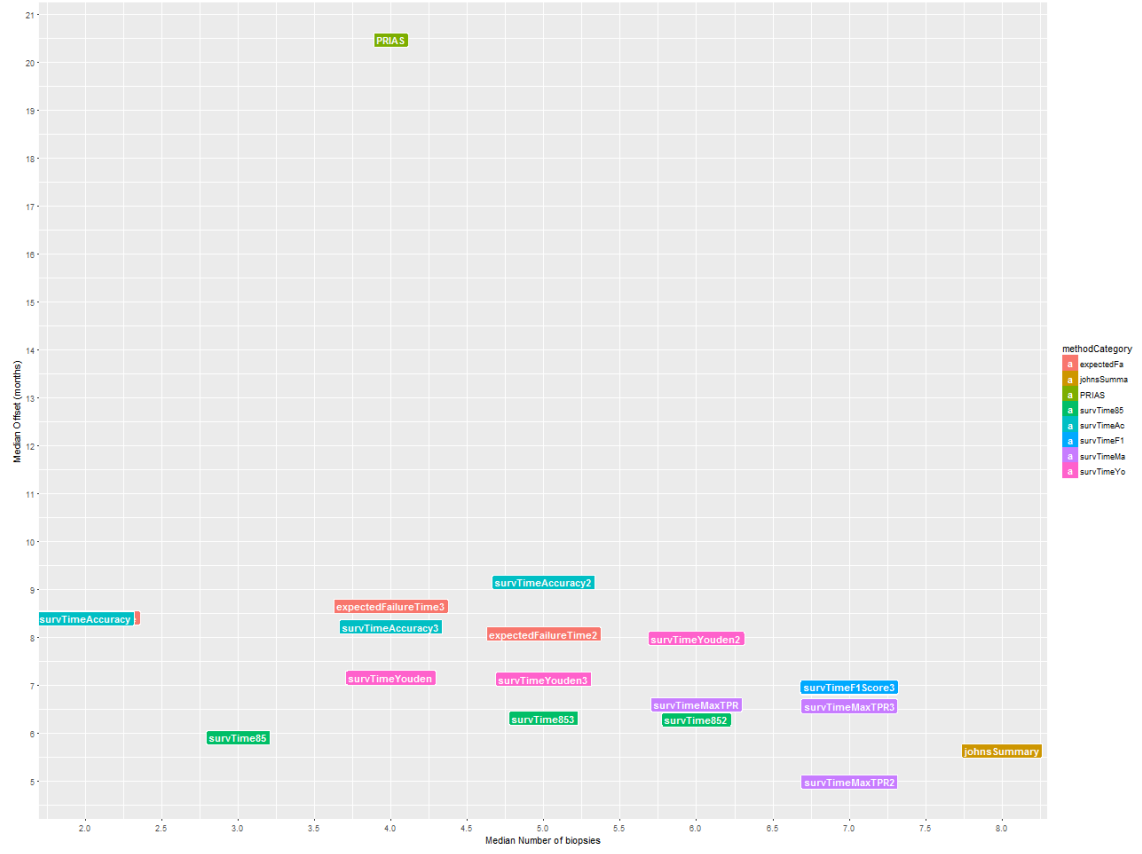
Figure 8: Median number of biopsies against the median offset (in years) for each of the approaches in scenario 1.
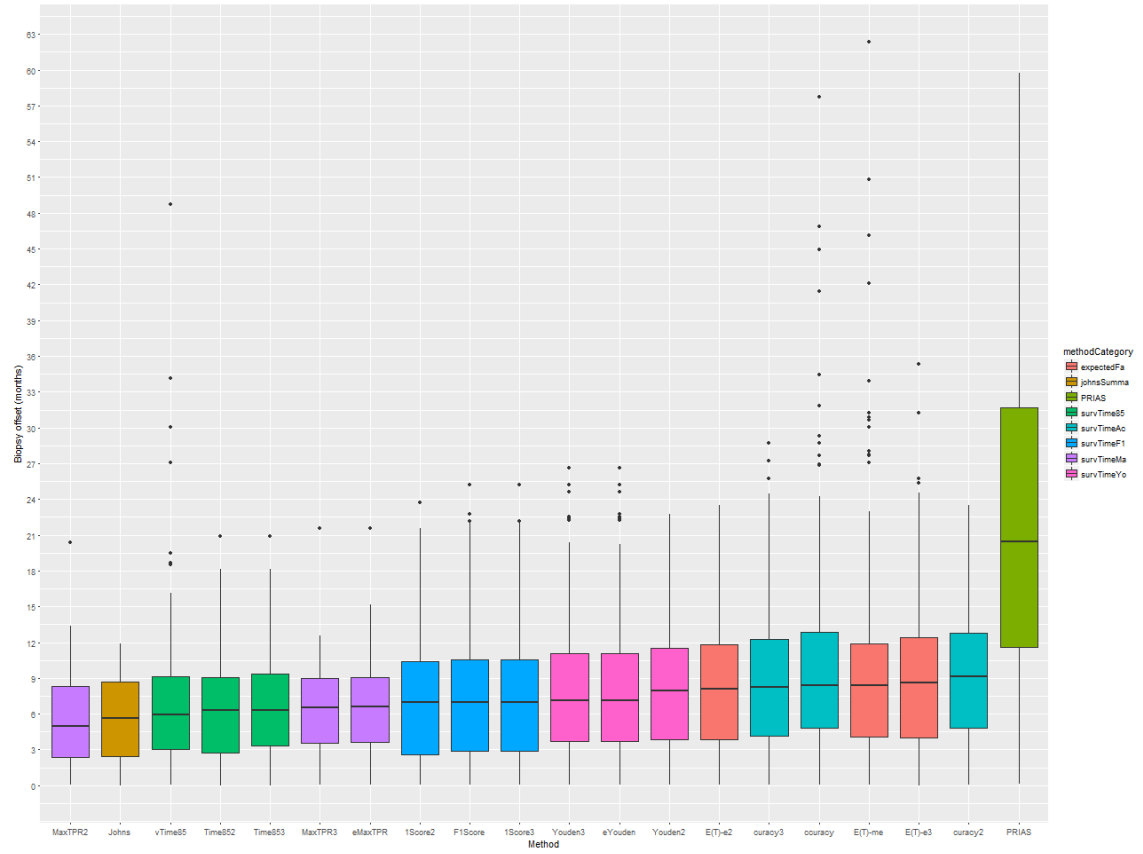
Figure 9: Boxplot for the offset corresponding to the various approaches in scenario 1.
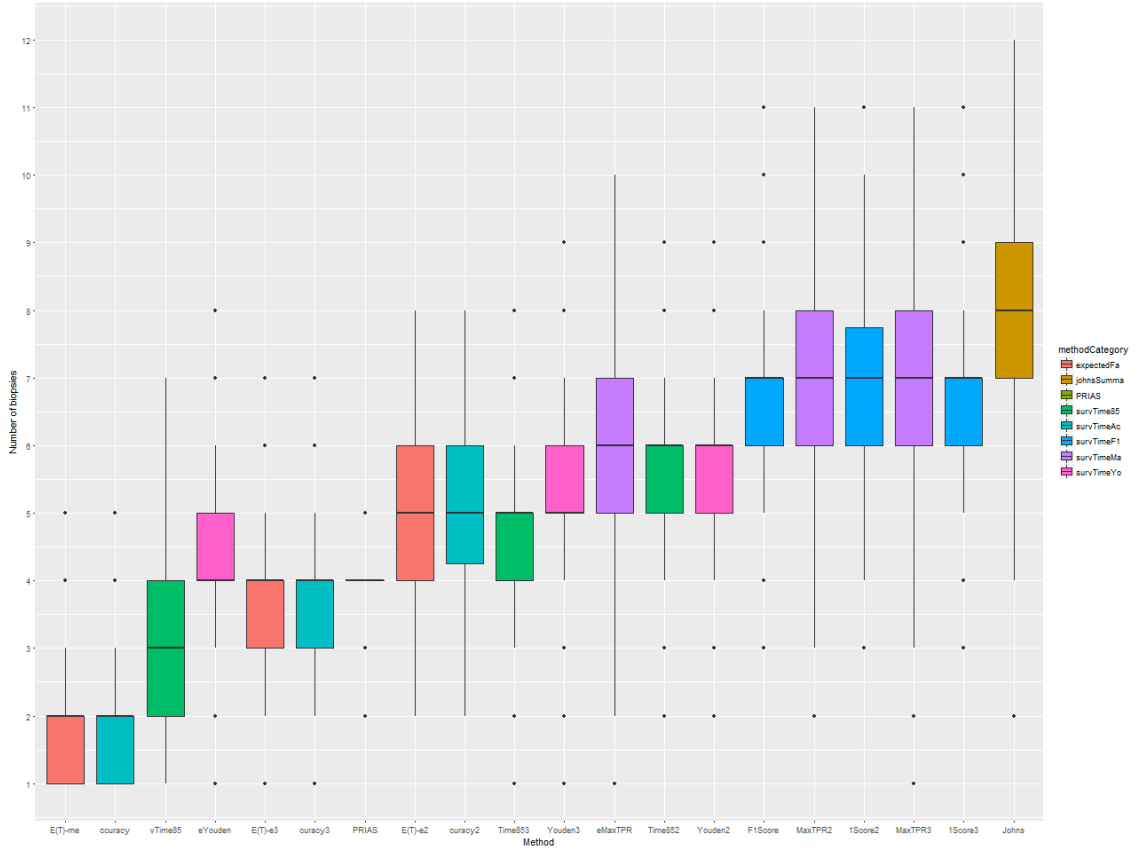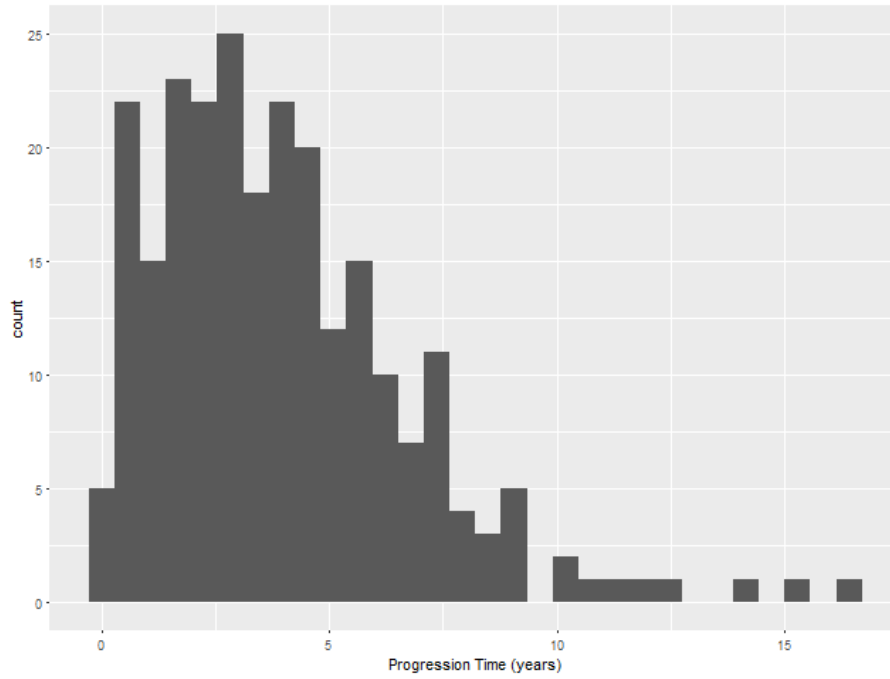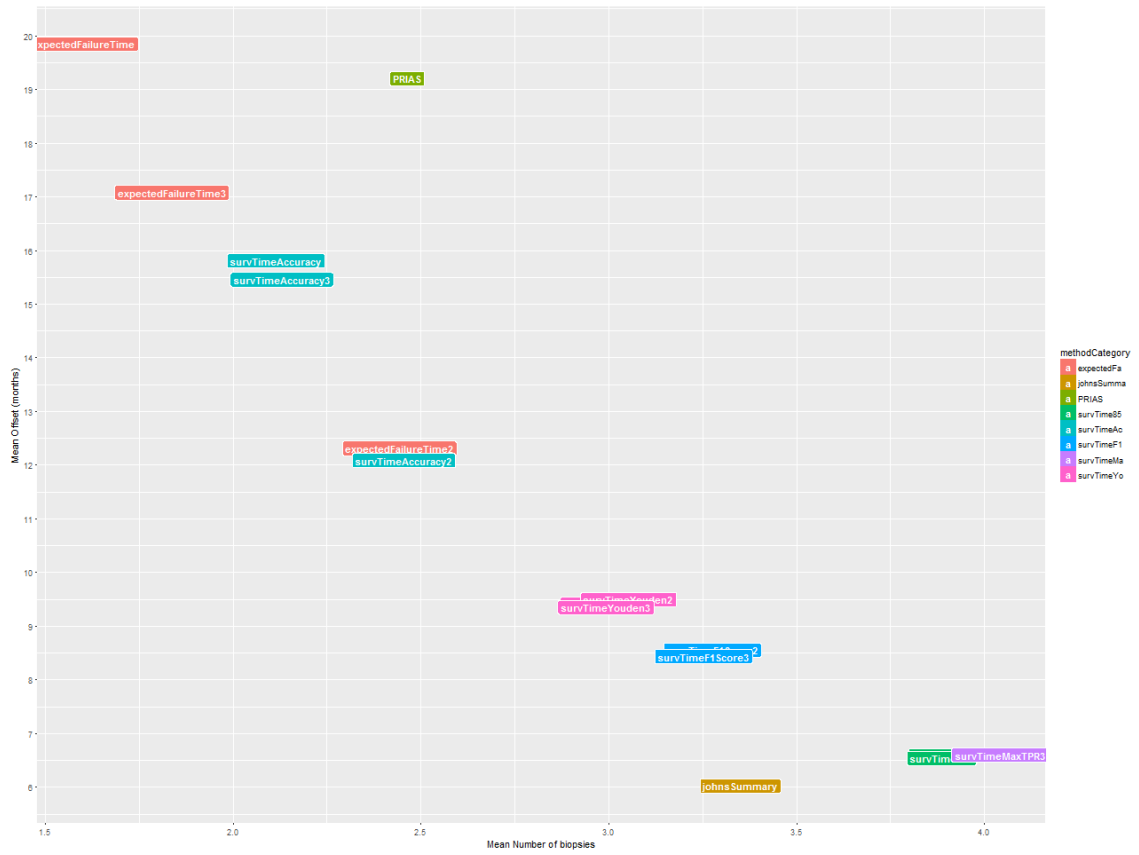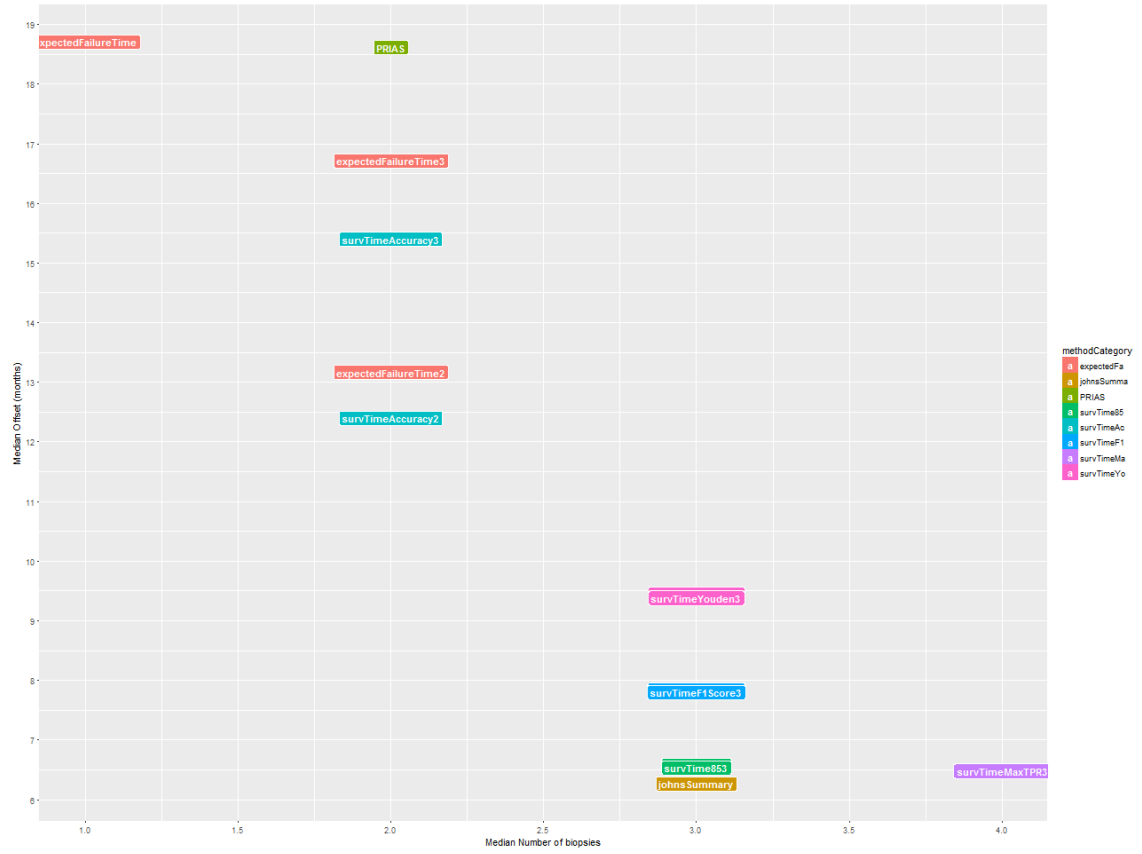
Figure 10: Boxplot for the number of biopsies corresponding to the various approaches in scenario 1.

5.3.2 Scenario 2

Unlike the previous scenario, the Gleason reclassification times for the patients in Scenario 2 are mostly between 0 and 5 years. The Gleason reclassification times of test patients from one of the data sets is shown in Figure 11. Figure 14 shows that, for this data set the approach with the least number of biopsies is conditional expected failure time. The mean and median number of biopsies are 1.5 and 1 respectively. While the mean and median offset is around 18 months, there is considerable variation in the offset for the various patients. The first and third quartiles are at 12 months and 27 months respectively. The large variation in offset is due to the fact that time to Gleason reclassification has larger variance since it is based on a small history of the patient. In such a scenario one might be inclined towards doing a biopsy every year as they have the least offset. However that approach leads to a very large number of biopsies as shown in Figure 15. Certain approaches based on dynamic risk perform better here, both in terms of number of biopsies as well as the offset. In particular if the choice of κ can be based on maximization of the Youden index or a fixed κ can be chosen.

Figure 11: Gleason reclassification times for patients from the test data set of scenario 2.

Figure 12: Mean number of biopsies against the mean offset (in years) for each of the approaches in scenario 2.

Figure 13: Median number of biopsies against the median offset (in years) for each of the approaches in scenario 2.
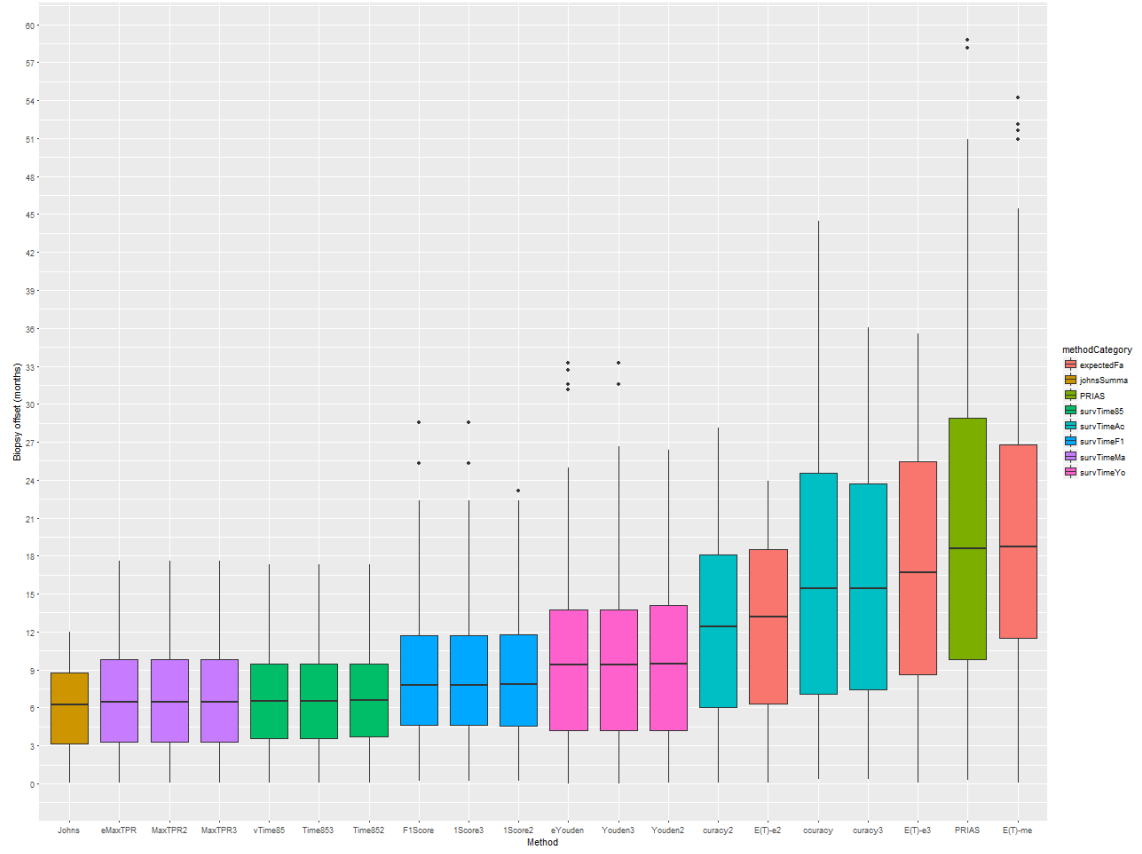
Figure 14: Boxplot for the offset corresponding to the various approaches in scenario 2.
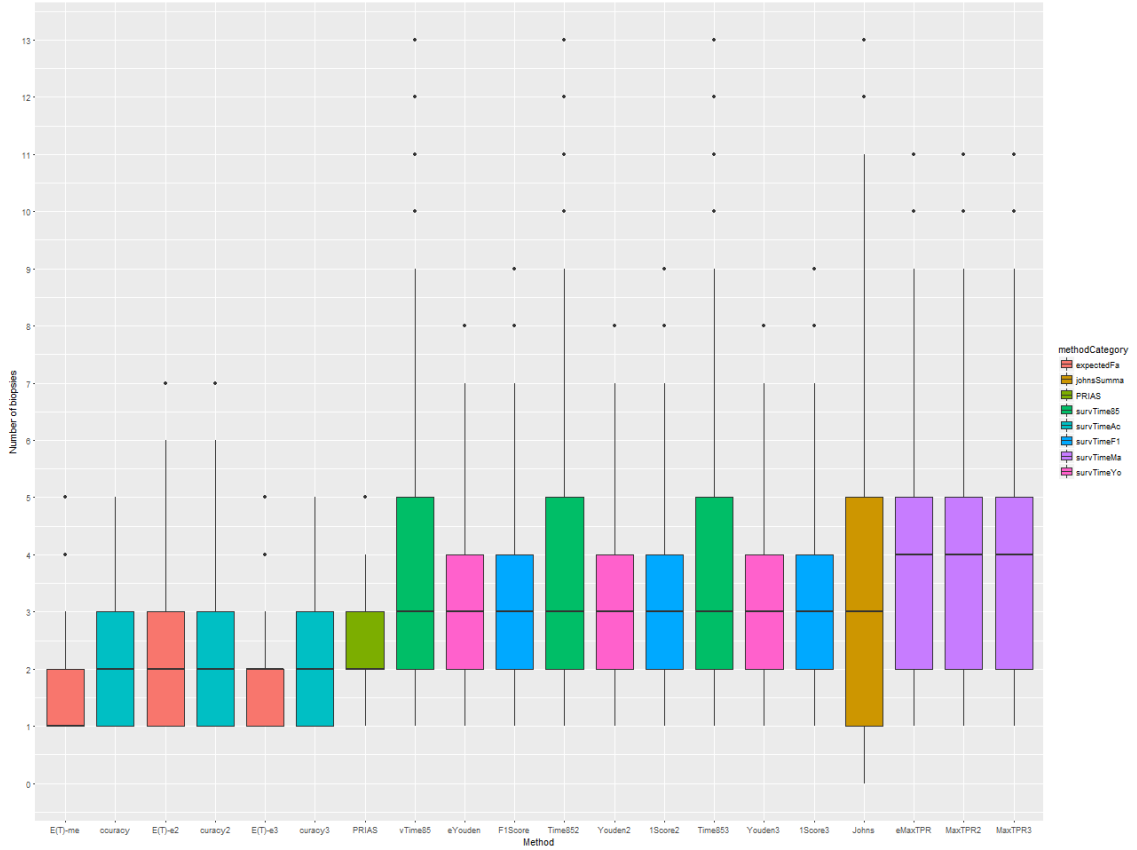
Figure 15: Boxplot for the number of biopsies corresponding to the various approaches in scenario 2.

5.3.3 Scenario 3

In scenario 3, the Gleason reclassification times for the patients are widely spread, mostly between 2 and 9 years. i.e. patients fail late as well early. The Gleason reclassification times of test patients from one of the data sets is shown in Figure 16. Figure 19 shows that, for this data set the approach with the least number of biopsies is conditional expected failure time. The mean and median number of biopsies are 1.5 and 1 respectively. This method also has considerable variation in the offset for the various patients. The first and third quartiles are at 9 months and 27 months respectively. A more detailed analysis revealed that the variation in offset was higher for subjects with earlier failure times. For e.g. the mean and median offset in subjects with reclassification times more than 4 years was nearly 13.5 months. For others it was nearly 39.5 months. This is once again is due to the fact that time to Gleason reclassification has larger variance since it is based on a small history of the patient. And thus usefulness of conditional expected failure time is questionable.

Dynamic risk based methods once again provide an alternative. If a fixed κ of 0.15 is used then although the offset will be low, there is very high variation in number of biopsies. i.e. people who have reclassifications early will benefit but people who have reclassifications later will have too many biopsies. If κ is chosen such that accuracy is maximized, and a biopsy is done whenever there is a gap of 2 years then a reasonable offset is obtained. The first and third quartiles are almost 4.5 and 18 months. The first and third quartiles for number of biopsies are 3 and 4.
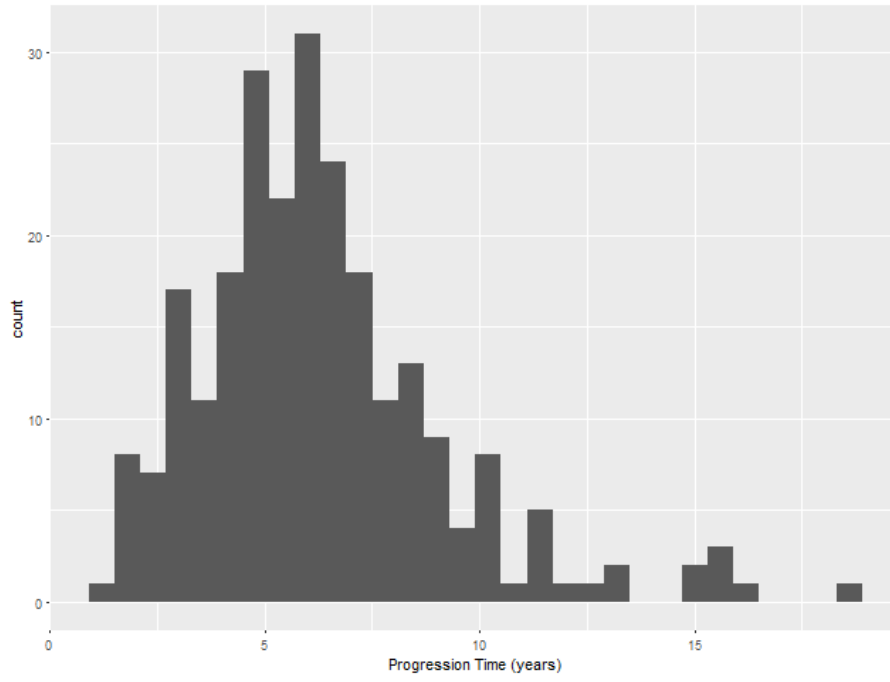
Figure 16: Gleason reclassification times for patients from the test data set of scenario 3.
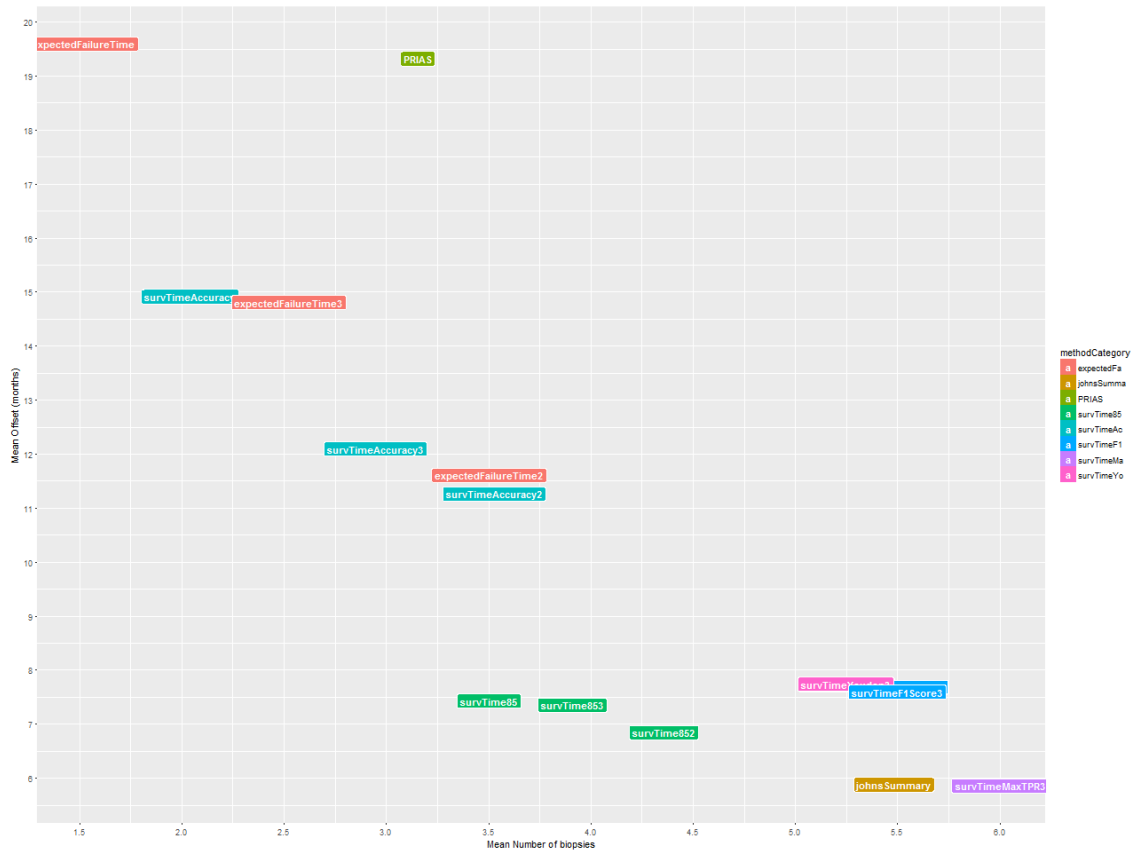

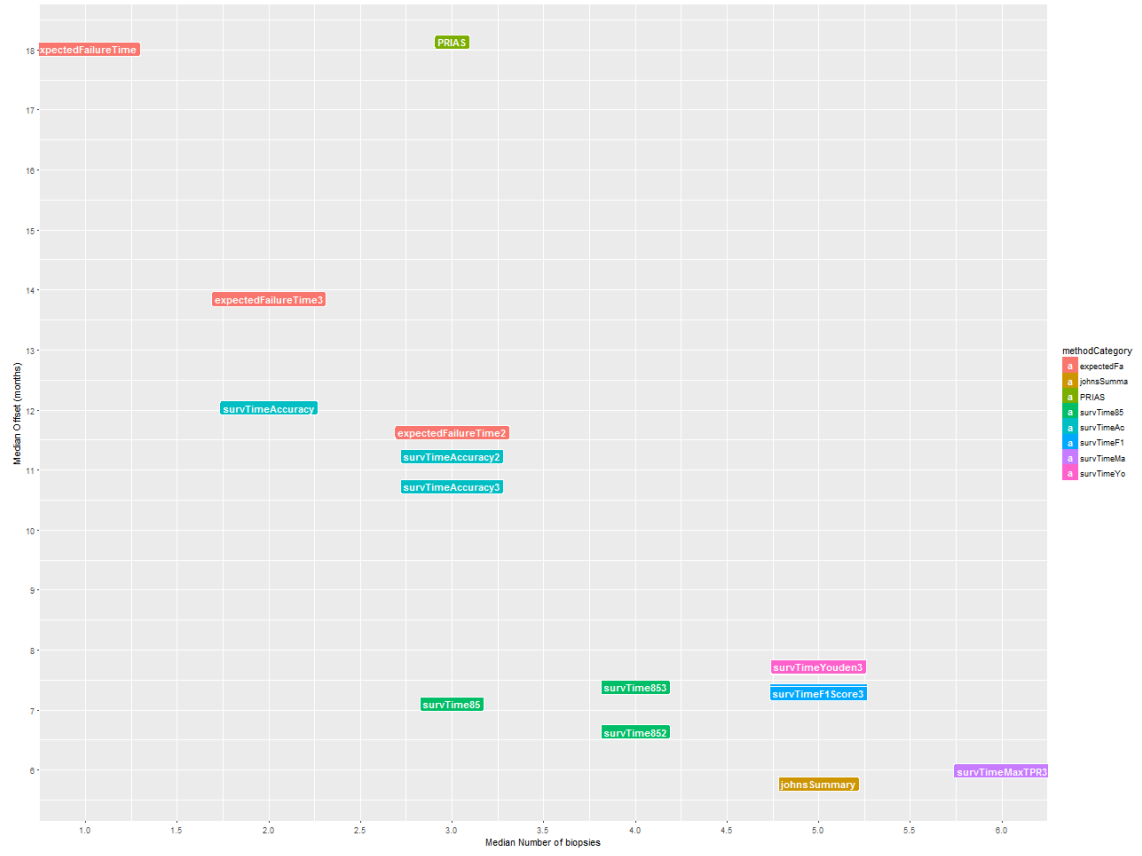Figure 17: Mean number of biopsies against the mean offset (in years) for each of the approaches in scenario 3.

Figure 18: Median number of biopsies against the median offset (in years) for each of the approaches in scenario 3.
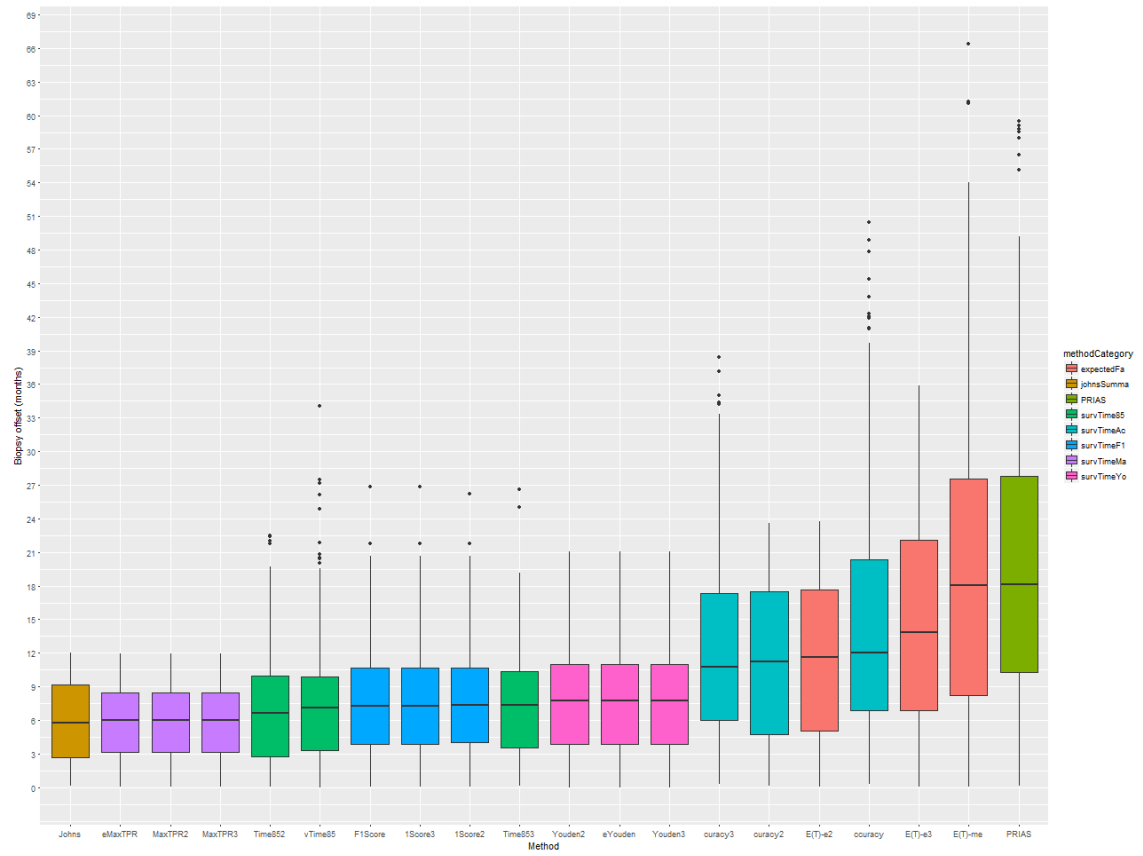
Figure 19: Boxplot for the offset corresponding to the various approaches in scenario 3.
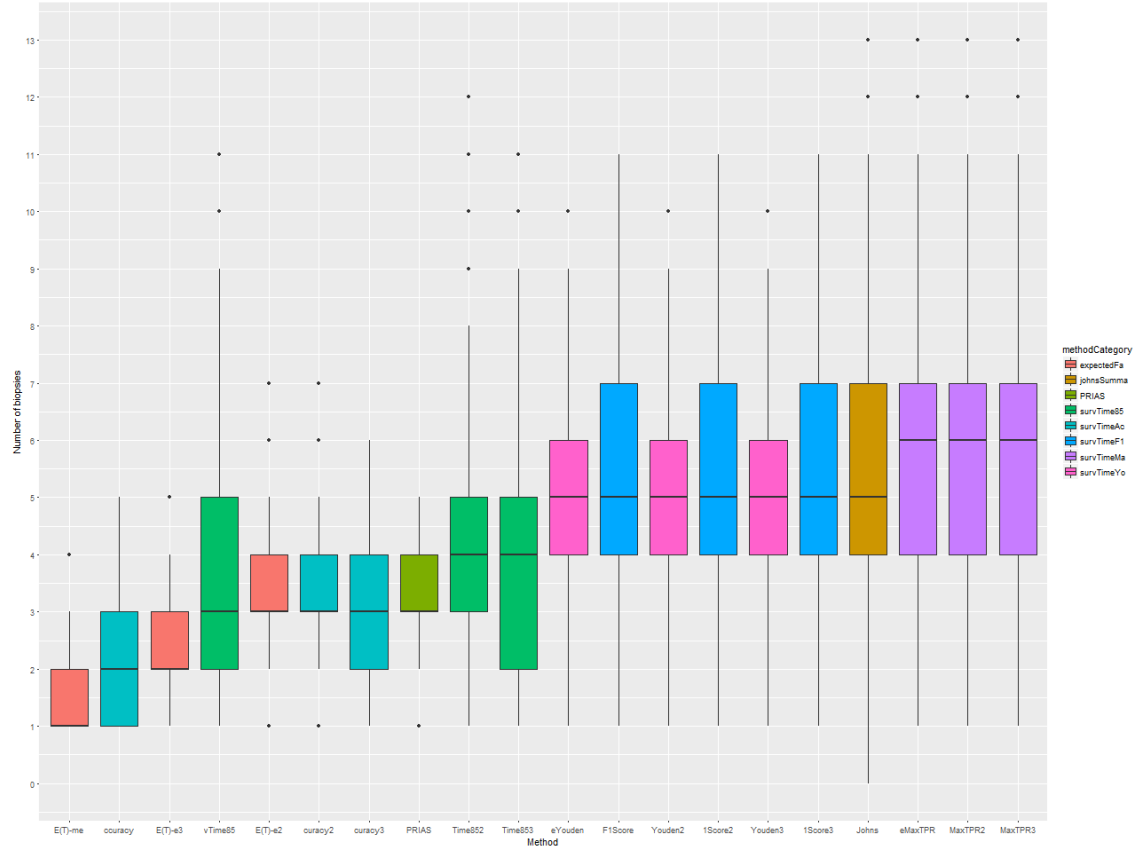
Figure 20: Boxplot for the number of biopsies corresponding to the various approaches in scenario 3.

References

Bebu, Ionut and John M. Lachin (2017). "Optimal screening schedules for disease progression with application to diabetic retinopathy". In: *Biostatistics*. DOI: 10.1093/biostatistics/kxv009.

Berger, James O (1985). *Statistical Decision Theory and Bayesian Analysis*. Springer Science & Business Media.

Bokhorst, Leonard P et al. (2015). "Compliance rates with the Prostate Cancer Research International Active Surveillance (PRIAS) protocol and disease reclassification in noncompliers". In: *European urology* 68.5, pp. 814–821.

Bokhorst, Leonard P et al. (2016). "A decade of active surveillance in the PRIAS study: an update and evaluation of the criteria used to recommend a switch to active treatment". In: *European Urology* 70.6, pp. 954–960.

Eilers, Paul HC and Brian D Marx (1996). "Flexible smoothing with B-splines and penalties". In: *Statistical science*, pp. 89–102.

Keegan, Kirk A et al. (2012). "Active surveillance for prostate cancer compared with immediate treatment". In: *Cancer* 118.14, pp. 3512–3518.

Loeb, Stacy et al. (2013). "Systematic review of complications of prostate biopsy". In: *European urology* 64.6, pp. 876–892.

López-Ratón, Mónica et al. (2014). "OptimalCutpoints: an R package for selecting optimal cutpoints in diagnostic tests". In: *Journal of Statistical Software* 61.8, pp. 1–36.

O'Mahony, James F et al. (2015). "The Influence of Disease Risk on the Optimal Time Interval between Screens for the Early Detection of Cancer: A Mathematical Approach". In: *Medical Decision Making* 35.2, pp. 183–195.

Parmigiani, Giovanni (1998). "Designing observation times for interval censored data". In: *Sankhyā: The Indian Journal of Statistics, Series A*, pp. 446–458.

Rizopoulos, Dimitris (2011). "Dynamic Predictions and Prospective Accuracy in Joint Models for Longitudinal and Time-to-Event Data". In: *Biometrics* 67.3, pp. 819–829.

— (2012). *Joint models for longitudinal and time-to-event data: With applications in R*. CRC Press.

— (2014). "The R package JMbayes for fitting joint models for longitudinal and time-to-event data using MCMC". In: *arXiv preprint arXiv:1404.7625*.

Rizopoulos, Dimitris et al. (2016). "Personalized screening intervals for biomarkers using joint models for longitudinal and survival data". In: *Biostatistics* 17.1, p. 149. DOI: 10.1093/biostatistics/kxv031. eprint: /oup/backfile/content_public/journal/biostatistics/17/1/10.1093_biostatistics_kxv031/3/kxv031.pdf.

Robert, Christian (2007). *The Bayesian choice: from decision-theoretic foundations to computational implementation*. Springer Science & Business Media.

Sokolova, Marina and Guy Lapalme (2009). "A systematic analysis of performance measures for classification tasks". In: *Information Processing & Management* 45.4, pp. 427–437.

Tosoian, Jeffrey J et al. (2011). "Active surveillance program for prostate cancer: an update of the Johns Hopkins experience". In: *Journal of Clinical Oncology* 29.16, pp. 2185–2190.

Tsiatis, Anastasios A and Marie Davidian (2004). "Joint modeling of longitudinal and time-to-event data: an overview". In: *Statistica Sinica*, pp. 809–834.

Welty, Christopher J et al. (2015). "Extended followup and risk factors for disease reclassification in a large active surveillance cohort for localized prostate cancer". In: *The Journal of urology* 193.3, pp. 807–811.

A   Appendix Heading

Lorem ipsum dolor sit amet, consectetur adipiscing elit. Suspendisse accumsan magna est, quis elementum leo laoreet eu. Donec sollicitudin elit non massa venenatis, in viverra dolor sagittis. Maecenas ac justo pulvinar, consectetur mauris hendrerit, vulputate lacus. Etiam tristique sapien quis sem commodo, et eleifend tortor viverra. In hac habitasse platea dictumst. Phasellus vel tempus risus, sit amet consectetur massa. Duis rutrum lectus eu ligula egestas iaculis. Sed condimentum, ipsum in dignissim condimentum, nisi turpis blandit massa, et aliquam magna ligula eget lacus. Donec ac eleifend nulla, quis cursus nisi. Lorem ipsum dolor sit amet, consectetur adipiscing elit. Suspendisse accumsan magna est, quis elementum leo laoreet eu. Donec sollicitudin

elit non massa venenatis, in viverra dolor sagittis. Maecenas ac justo pulvinar, consectetur mauris hendrerit, vulputate lacus. Etiam tristique sapien quis sem commodo, et eleifend tortor viverra. In hac habitasse platea dictumst. Phasellus vel tempus risus, sit amet consectetur massa. Duis rutrum lectus eu ligula egestas iaculis. Sed condimentum, ipsum in dignissim condimentum, nisi turpis blandit massa, et aliquam magna ligula eget lacus. Donec ac eleifend nulla, quis cursus nisi.